


# APPENDIX E FCT DOCUMENT COVER SHEET <sup>1</sup>

Name/Title of Deliverable/Milestone/  
Revision No. DPC Disposal Thermal Scoping Analysis

Work Package Title and Number Technical and Programmatic Solutions for Direct Disposal of  
DPCs – SNL (SF-21SN01030505)

Work Package WBS Number WBS 1.08.01.03.05

Responsible Work Package Manager Ernest Hardin   
(Name/Signature)

Date Submitted

Quality Rigor Level for Deliverable/Milestone <sup>2</sup>	<input type="checkbox"/> QRL-1	<input type="checkbox"/> QRL-2	<input type="checkbox"/> QRL-3	<input checked="" type="checkbox"/> QRL-4
	<input type="checkbox"/> Nuclear Data			Lab- Specific

This deliverable was prepared in accordance with Sandia National Laboratories  
(Participant/National Laboratory Name)

QA program which meets the requirements of  
 DOE Order 414.1     NQA-1-2000     Other

**This Deliverable was subjected to:**

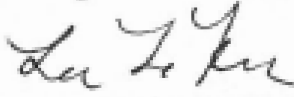
<input checked="" type="checkbox"/> Technical Review	<input type="checkbox"/> Peer Review
<b>Technical Review (TR)</b>	<b>Peer Review (PR)</b>
<b>Review Documentation Provided</b>	<b>Review Documentation Provided</b>
<input type="checkbox"/> Signed TR Report or,	<input type="checkbox"/> Signed PR Report or,
<input type="checkbox"/> Signed TR Concurrence Sheet or,	<input type="checkbox"/> Signed PR Concurrence Sheet or,
<input checked="" type="checkbox"/> Signature of TR Reviewer(s) below	<input type="checkbox"/> Signature of PR Reviewer(s) below

**Name and Signature of Reviewers**  
Tara LaForce/SNL

---



---



---



---

**NOTE 1:** Appendix E should be filled out and submitted with the deliverable. Or, if the PICS:NE system permits, completely enter all applicable information in the PICS:NE Deliverable Form. The requirement is to ensure that all applicable information is entered either in the PICS:NE system or by using the FCT Document Cover Sheet

- In some cases there may be a milestone where an item is being fabricated, maintenance is being performed on a facility, or a document is being issued through a formal document control process where it specifically calls out a formal review of the document. In these cases, documentation (e.g., inspection report, maintenance request, work planning package documentation or the documented review of the issued document through the document control process) of the completion of the activity, along with the Document Cover Sheet, is sufficient to demonstrate achieving the milestone.

**NOTE 2:** If QRL 1, 2, or 3 is not assigned, then the QRL 4 box must be checked, and the work is understood to be performed using laboratory specific QA requirements. This includes any deliverable developed in conformance with the respective National Laboratory / Participant, DOE or NNSA-approved QA Program.

# **DPC Disposal Thermal Scoping Analysis**

## **Spent Fuel and Waste Disposition**

*Prepared for  
US Department of Energy  
Spent Fuel and Waste Science and Technology  
by  
P. Jones, K.-W. Chang and E. Hardin  
Sandia National Laboratories, Albuquerque, NM*

*M4SF-21SN010305055  
SAND2021-7515 R  
June 2021*

## Revision History

<p><b>Deliverable:</b> M4SF-21SN010305055 <b>Title:</b> <i>DPC Disposal Thermal Scoping Analysis</i> <b>Work Package:</b> Technical and Programmatic Solutions for Direct Disposal of DPCs – SNL (SF-21SN01030505) <b>WBS:</b> 1.08.01.03.05 Direct Disposal of Dual Purpose Canisters</p>	<p>Prepared at Sandia, with technical review by Tara LaForce, compliant with NFCSC/ SFWD QAPD Rev. 6, Appendix B. The Sandia formal review &amp; approval (SAND2021- 7515 R) was for unlimited release, and the resulting copy was submitted to PICS/NE in satisfaction of the deliverable.</p>
--	---

NOTICE: This report was prepared as an account of work sponsored by an agency of the United States Government. Neither the United States Government, nor any agency thereof, nor any of their employees, nor any of their contractors, subcontractors, or their employees, make any warranty, express or implied, or assume any legal liability or responsibility for the accuracy, completeness, or usefulness of any information, apparatus, product, or process disclosed, or represent that its use would not infringe privately owned rights. Reference herein to any specific commercial product, process, or service by trade name, trademark, manufacturer, or otherwise, does not necessarily constitute or imply its endorsement, recommendation, or favoring by the United States Government, any agency thereof, or any of their contractors or subcontractors. The views and opinions expressed herein do not necessarily state or reflect those of the United States Government, any agency thereof, or any of their contractors.

Sandia National Laboratories is a multimission laboratory managed and operated by National Technology and Engineering Solutions of Sandia LLC, a wholly owned subsidiary of Honeywell International Inc. for the U.S. Department of Energy's National Nuclear Security Administration under contract DE-NA0003525.



### **Disclaimer**

This report does not take into account contractual limitations or obligations under the Standard Contract for Disposal of Spent Nuclear Fuel and/or High-Level Radioactive Waste (Standard Contract) (10 CFR Part 961). For example, under the provisions of the Standard Contract, spent nuclear fuel in multi-assembly canisters is not an acceptable waste form, absent a mutually agreed to contract amendment.

To the extent discussions or recommendations in this report conflict with the provisions of the Standard Contract, the Standard Contract governs the obligations of the parties, and this report in no manner supersedes, overrides, or amends the Standard Contract.

This report reflects technical work which could support future decision making by DOE. No inferences should be drawn from this report regarding future actions by DOE, which are limited both by the terms of the Standard Contract and Congressional appropriations for the Department to fulfill its obligations under the Nuclear Waste Policy Act including licensing and construction of a spent nuclear fuel repository.

## Table of Contents

Abstract.....	viii
Acknowledgments.....	ix
Abbreviations.....	ix
<b>1. Introduction .....</b>	<b>1-1</b>
<b>2. Semi-Analytical Model.....</b>	<b>2-1</b>
2.1 Results Summary .....	2-3
<b>3. Thermal Creep Model for a Salt Repository.....</b>	<b>3-1</b>
3.1 Reference Case.....	3-2
3.2 Grid Size and Resolution Studies .....	3-7
3.3 Comparison of FLAC 2D Model with Semi-Analytical 3D Model, Peak Temperature .....	3-9
3.4 “Calibration” of the 2D Line Source to Match 3D Peak Temperature at the Drift Wall .....	3-11
3.5 Temperature and Displacement Histories for Percentile DPCs .....	3-12
3.6 Summary and Recommendations for Thermal-Creep Modeling of Salt .....	3-15
<b>4. PFLOTRAN Repository Model.....</b>	<b>4-1</b>
4.1 Natural Barrier System (Host Rock).....	4-1
4.2 Engineered Barrier System .....	4-4
4.3 Waste Package .....	4-5
4.4 Numerical Model Setting.....	4-5
4.4.1 Model Domain .....	4-5
4.4.2 Parameters.....	4-6
4.5 Results.....	4-9
<b>5. Summary and Recommendations .....</b>	<b>5-1</b>
<b>6. References.....</b>	<b>6-1</b>

## List of Tables

Table 1-1. DPCs selected to represent percentiles of heat output. ....	1-2
Table 1-2. Histories of heat output for representative DPCs (from UNF-ST&DARDS).....	1-3
Table 1-3. DPC dimensions (discuss assumed overpack thickness) .....	1-4
Table 1-4. Thermal properties for generic host media.....	1-5
Table 1-5. Repository dimensions and other concept data for generic host media. ....	1-6
Table 2-1. Geometry and near-field properties for semi-analytical model.....	2-2
Table 2-2. Results summary for percentiles of heat output and different disposal concepts using wet thermal conductivities. ....	2-3
Table 3-1. Summary of 2D line-load “calibration” exercise. ....	3-11
Table 4-1. Material parameters for PFLOTRAN modeling. ....	4-7

## List of Figures

Figure 2-1.	Schematic of semi-analytical model elements superimposed.....	2-2
Figure 2-2.	Comparison of waste package overpack surface temperature histories with dry and wet backfill/buffer, for the clay/shale repository concept with 10 <sup>th</sup> percentile heating. ....	2-4
Figure 2-3.	Comparison of waste package overpack surface temperature histories with dry and wet backfill/buffer, for the clay/shale repository concept with 50 <sup>th</sup> percentile heating. ....	2-4
Figure 3-1.	Cross-plot between $K_{th}$ values (functions of temperature) calculated using the fit from Bechthold et al. (2004), and the intrinsic FLAC <i>th_general</i> function. ....	3-2
Figure 3-2.	Reference case temperature histories at three locations on the drift wall, as noted.....	3-3
Figure 3-3.	Reference case y-displacement histories at three locations on the drift wall, as noted.....	3-3
Figure 3-4.	Reference case temperature histories (similar to Figure 3-2 but greater vertical extent).....	3-5
Figure 3-5.	Temperature histories with creep turned off, and $K_{th}$ dependent on temperature. Compare to Figure 3-4. ....	3-5
Figure 3-6.	Histories of drift wall temperature (left) and displacements (right) with $E_A$ increased 20% (creep rate multiplier 0.034 at 373 K, 0.069 at 473 K). Compare to Figure 3-4. ....	3-6
Figure 3-7.	Histories of drift wall temperature (left) and displacements (right) with $E_A$ increased 30% (creep rate multiplier 0.0062 at 373 K, 0.018 at 473 K). Compare to Figure 3-4. ....	3-6
Figure 3-8.	Grid resolution study comparing drift-wall temperatures (lower) for grid resolution of 1 m, 0.5 m, and 0.25 m (upper, excerpted from the larger $\pm 150$ m model grids). Temperature histories for 300 yr are shown in the lower plots, for grid resolution of 1 m, 0.5 m, and 0.25 m (left to right). Cases were run using 99 <sup>th</sup> percentile heating, fixed intact salt and backfill $K_{th}$ , and no creep. ....	3-8
Figure 3-9.	Benchmark line-source runs with the semi-analytical model implemented in MathCad (upper), and a similar 2D FLAC model (lower).....	3-10
Figure 3-10.	“Calibration” of 2D FLAC line-load thermal model to 3D semi-analytical model implemented in MathCad. ....	3-11
Figure 3-11.	Temperature (upper) and y-displacement (lower) for “calibrated” cases with 99 <sup>th</sup> (left) and 90 <sup>th</sup> (right) percentile heating. ....	3-13
Figure 3-12.	Temperature (upper) and y-displacement (lower) for “calibrated” cases with 50 <sup>th</sup> (left) and 10 <sup>th</sup> (right) percentile heating. ....	3-14

Figure 4-1.	Conceptual model of unsaturated alluvium case (after Mariner et al. 2018). The near-field model in this study focuses on the upper UZ portion where the infiltration through the surface is dominant. ....	4-3
Figure 4-2.	Model domain and grid setting. Four sections are modeled: waste package (dark red), backfill/buffer (red), DRZ (yellow), and host rock (blue). ....	4-5
Figure 4-3.	Model geometry of four types of repositories. The center of the waste package for shale, crystalline, and salt rock repositories are located at depth of 500m, whereas one for unsaturated alluvium case is located at depth of 250m and the domain top extends to the surface. ....	4-6
Figure 4-4.	Initial conditions for unsaturated alluvium case. ....	4-9
Figure 4-5.	Results for the 90 <sup>th</sup> percentile DPC heat source: (A to C) temperature; (D to F) liquid pressure; and (G to I) gas pressure and saturation. ....	4-10
Figure 4-6.	Results for the 50 <sup>th</sup> percentile DPC heat source: (A to C) temperature; (D to F) liquid pressure; and (G to I) gas pressure and saturation. ....	4-11
Figure 4-7.	Odd behaviors of flow within unstructured grids: gas saturation. ....	4-12



## **Deliverable Description**

Collaborate with GDSA staff to define thermal history cases for analysis, including representative as-loaded DPC thermal power histories, EBS design concepts, thermal properties for all materials, and backfill behavior (hydration and consolidation). Perform scoping analyses using a semi-analytical tool, and perform a coupled thermomechanical simulation of a salt repository (with creep closure, temperature effect on  $K_{th}$ , and backfill consolidation). Produce a M4 deliverable summarizing the work.

### **Abstract**

This is a progress report on thermal modeling for DPC direct disposal that covers several available calculation methods and addresses creep and temperature-dependent properties in a salt repository. Three modeling approaches are demonstrated:

- A semi-analytical calculation method that uses linear solutions with superposition and imaging, to represent a central waste package in a larger array.
- A finite difference model of coupled thermal creep, implemented in FLAC2D.
- An integrated finite difference thermal-hydrologic modeling approach for repositories in different generic host media, implemented in PFLOTRAN.

These approaches are at different levels of maturity, and future work is expected to add refinements and establish the best applications for each.

The principal finding from this study is that the near-field temperatures at or near DPC-based waste packages are much lower than previous studies have suggested. This is because the present study exclusively uses thermal output projections for as-loaded DPCs from the UNF-ST&DARDS database, whereas previous studies have used bounding assumptions such that all waste packages contain high-burnup fuel. This finding requires that waste package emplacement in a repository begin at or around calendar 2100, so that each DPC ages about 100 yr before disposal.

Recommendations for future work are presented, including model improvements and sensitivity studies, and studies with alternative DPC aging/emplacement schedules.

It is anticipated that after some further development, these models will be used to develop high-confidence thermal histories for the outer surfaces of DPC-based waste packages. These would then be used as boundary conditions for internal heat transfer models of the DPCs, to develop histories for fuel rods and other components after disposal.

## Acknowledgments

The Sandia lead for this report was Ernest Hardin, who authored Sections 1, 3 and 5. Section 2 was contributed by Phil Jones, and Section 4 by Kyung Won Chang, both of Sandia. Tara LaForce of Sandia helped to guide the project, and performed the technical review. Kaushik Banerjee of PNNL provided the UNF-ST&DARDS data and calculations of DPC heat output.

## Abbreviations

2D	Two-dimensional
3D	Three-dimensional
BWR	Boiling water reactor
DPC	Dual-purpose canister
DRZ	Disturbed rock zone
EBS	Engineered barrier system
$K_{th}$	Thermal conductivity
PWR	Pressurized water reactor
SNF	Spent nuclear fuel

## **1. Introduction**

This report is intended to kick off a longer term effort to improve thermal predictions for direct disposal of commercial spent nuclear fuel (SNF) in dual-purpose canisters (DPCs). Previous studies have established that DPCs can be disposed of in various generic (non-site specific) geologic media without exceeding emplacement temperature power limits proposed for those media, in reasonable timeframes for repository operations (Hardin et al. 2015). For example, with temperature-resistant geologic media such as unsaturated hard rock or salt, underground emplacement of waste packages could commence right away and be completed sometime in the mid-2100's. For other media such as clay or shale, emplacement power limits are estimated to be lower. DPCs would continue to be aged, and emplacement could begin around calendar 2100 and continue for approximately 100 years to repository closure (Stein et al. 2020).

The greatest thermal management challenge would be meeting the lower power limits needed for disposal concepts that rely heavily on a clay buffer or clay-based backfill for waste isolation, such as the crystalline concept (hydrologically saturated). Clays can be mineralogically altered by heat and circulating moisture, particularly in a thermal gradient. This could change the materials in ways that allow radionuclides from breached waste packages to be released faster and in greater quantities to the surrounding host rock. Studies of clay resistance to alteration at higher temperatures are underway (Stein et al. 2020). When such studies mature, there will be a need to compare the resulting thermal limits with predictions for DPC-based waste packages.

To limit the peak temperature in a clay buffer or clay-based backfill, previous studies have suggested that some DPCs might be aged at the surface until 2200 or beyond (Hardin 2013; Hardin et al. 2012a, 2014). These studies were done to establish the general feasibility and timeframe for DPC direct disposal, without including complicating factors such as buffer hydration, creep consolidation, and temperature dependence of physical properties such as thermal conductivity.

A recent clay repository concept study (Stein et al 2020, Section 4.5) used various scoping calculations to show how heat output from 21-PWR/44-BWR size waste packages could be managed to meet thermal objectives. The approach did not use heat output data from real DPCs, but instead used idealized waste packages that contain fuel assemblies with the same characteristics (enrichment, burnup, heat output). This allowed waste packages containing high-burnup fuel to have unrealistically high heat output, much greater than real DPCs in the current inventory. By the same token, waste packages modeled to contain only low burnup fuel have unrealistically low heat output.

Realistic heat output data is the first requirement for improved repository thermal modeling, especially for disposal concepts that are sensitive to heating of a clay buffer material or clay-based backfill. Secondly, a suite of models is needed that represent heat transfer and repository evolution with various degrees of fidelity. In this way, particular thermal management problems can be paired with modeling approaches that involve commensurate computational effort. Such a suite of models is the subject of this report and follow-on development activities that may proceed over the next few years.

### **Realistic DPC Thermal History Data**

Characteristics of as-loaded DPCs and the fuel they contain are compiled in the UNF-ST&DARDS database and associated software tools (Banerjee et al. 2016; Clarity et al. 2017). Of the roughly 3,200 DPCs that have been loaded so far in the U.S., 1,981 of them were available in UNF-

ST&DARDS. The database records fuel type, enrichment, average burnup by assembly, and discharge date among other parameters. The ORIGEN code is used to evaluate radionuclide composition out-of-reactor and after aging, and thus calculates heat generation also.

For this application, the heat output of 1,981 as-loaded DPCs in calendar 2100, 2200 and 2500 was obtained from UNF-ST&DARDS. DPCs representing percentiles of the frequency distribution of heat outputs (10<sup>th</sup>, 50<sup>th</sup>, 75<sup>th</sup>, 90<sup>th</sup>, 95<sup>th</sup> and 99<sup>th</sup>) were determined. The DPCs associated with these percentiles in 2100 were not always found to be at the same percentiles in calendar 2200 or 2500 because of difference in decay rates (Table 1-1). However, the differences were a few percent at most, with the hottest DPCs in 2100 decaying slightly faster than the hottest DPCs in later years (spreadsheets: *2100.xlsx*, *2200.xlsx* and *2500.xlsx*). Hence, the percentile DPCs from calendar 2100 were selected for thermal analysis of periods ranging from 300 to 1,000 years after emplacement (Table 1-2). Dimensions of these DPCs are given in Table 1-3.

Table 1-1. DPCs selected to represent percentiles of heat output.

Nominal Percentiles	DPC ID	Rank Order of Heat Output (of 1,981 DPCs) in Calendar Year:		
		2100	2200	2500
99 <sup>th</sup>	CR3-32PTH1-L-2D-W-13	1 (max.)	3	9
95 <sup>th</sup>	MPC-89_4803D_MPCFW045	98	152	204
90 <sup>th</sup>	DSC-32PTH_1803D_32PTH-032-C-1	198	240	263
75 <sup>th</sup>	MPC-32-MPC-224	495	521	526
50 <sup>th</sup>	MPC-24-MPC-003	990	1020	1057
10 <sup>th</sup>	24PT1_4701D_DSC009	1783	1787	1801

Table 1-2. Histories of heat output for representative DPCs (from UNF-ST&DARDS).

Calendar	99th (Watts)	95th (Watts)	90th (Watts)	75th (Watts)	50th (Watts)	10th (Watts)
2100	8,034	6,764	6,058	5,006	4,034	2388
2110	7,353	6,159	5,570	4,611	3,744	2239
2130	6,317	5,249	4,828	4,009	3,297	2006
2150	5,583	4,614	4,303	3,583	2,975	1834
2170	5,045	4,156	3,919	3,271	2,735	1704
2200	4,465	3,673	3,506	2,934	2,470	1557
2250	3,829	3,156	3,051	2,563	2,170	1384
2300	3,399	2,813	2,740	2,307	1,957	1257
2400	2,814	2,350	2,303	1,945	1,653	1071
2500	2,409	2,029	1,989	1,683	1,431	932
2750	1,749	1,504	1,459	1,236	1,055	693
3000	1,339	1,177	1,123	952	815	539
3500	882	810	745	631	545	366
4000	668	636	567	481	418	284
5000	506	502	433	367	321	223
6000	449	451	385	327	286	201
8000	388	393	333	283	248	176
10000	342	348	294	250	219	158
15000	256	264	220	189	165	123
20000	199	207	171	147	128	98
30000	131	138	113	97	85	67
40000	94	99	81	70	61	49
60000	56	58	47	41	35	29
80000	37	37	31	27	23	18
100000	27	26	22	19	16	13
150000	19	16	14	12	10	7
200000	17	14	13	11	9	6
300000	16	13	12	10	9	6
400000	15	12	11	10	8	6
500000	14	11	11	9	8	5
750000	11	9	9	8	6	4
1000000	10	8	8	7	6	4
<b>Selected DPCs:</b>						
	<b>Location</b>	<b>DPC ID</b>		<b>Loaded Date</b>		
99th:	Crystal River ISFSI	CR3-32PTH1-L-2D-W-13		06/01/07		
95th:	Browns Ferry ISFSI	MPC-89_4803D_MPCFW045		06/08/17		
90th:	Turkey Point ISFSI	DSC-32PTH_1803D_32PTH-032-C-1		10/26/11		
75th:	Waterford ISFSI	MPC-32-MPC-224		04/01/12		
50th:	Arkansas Nuclear ISFSI	MPC-24-MPC-003		12/13/03		
10th:	San Onofre ISFSI	24PT1_4701D_DSC009		12/01/03		

Table 1-3. DPC dimensions (discuss assumed overpack thickness)

	DPC ID	DPC Dimensions				Waste Package	
		Length (in)	Dia. (in)	Length (m)	Radius (m)	Length (m)	Radius (m)
99th	CR3-32PTH1-L-2D-W-13	193.00	69.75	4.902	0.886	5.042	0.956
95th	MPC-89_4803D_MPCFW045	190.00	75.50	4.826	0.959	4.966	1.029
90th	DSC-32PTH_1803D_32PTH-032-C-1	193.00	69.75	4.902	0.886	5.042	0.956
75th	MPC-32-MPC-224	190.31	68.50	4.834	0.870	4.974	0.940
50th	MPC-24-MPC-003	190.31	68.50	4.834	0.870	4.974	0.940
10th	24PT1_4701D_DSC009	186.50	67.19	4.737	0.853	4.877	0.923
Assumed disposal overpack thickness 7 cm.							

### General Assumptions

1. Repository emplacement begins calendar 2100. DPC storage at the surface is monitored to maintain safety for at least 100 years, which corresponds approximately to calendar 2200. This offers sufficient aging that a robust program of emplacement could begin for any of the generic media considered in this report.
2. Neighboring waste packages have 75<sup>th</sup> percentile heat output. This is applicable to the FLAC and PFLOTRAN models which use symmetry to model a cell in a repository consisting of identical packages. Hence for these models, a representative result is obtained using the 75<sup>th</sup> percentile waste package (assuming an array of like packages in the far field). For the semi-analytical (MathCad) model 75<sup>th</sup> percentile packages can be put in the far field while any packages can be put in the near field. Using the 75<sup>th</sup> instead of the 50<sup>th</sup> percentile is a measure of conservatism that will increase temperatures slightly after time has transpired.
3. Future inventory will have similar fuel characteristics and DPC loading criteria, so that existing as-loaded thermal projections based on the UNF-ST&DARDS database are reasonably representative.
4. Heat generation is uniform within DPCs (all model and media).
5. Heat is generated by radioactive decay only, not criticality.
6. Geotemperature gradient is included by specifying constant top and bottom model temperatures (semi-analytical and PFLOTRAN models).
7. Host media thermal properties from Table 1-4 are used where possible.
8. Repository geometry and disposal concept details shown in Table 1-5 are used in the models where consistent with modeling constraints.

Table 1-4. Thermal properties for generic host media.

		$K_{th}$ (W/m-K)			Heat Capacity (J/kg-K)	Dry Bulk Density (kg/m <sup>3</sup> )	Volumetric Heat Capacitance (J/m <sup>3</sup> -K)
		Low	High	Average			
<b>Salt</b>	200C	4.4	5.4	4.88	927	2180	2.02e+06
	100C	2.7	3.7	3.21			
<b>Clay/Shale</b>		1.1	2.3	1.73	1005		
<b>Alluvium</b>	Unsat.	1	1.2	1.06	959	1525	1.46e+06
	Sat.	1.2	1.8	1.49			
<b>Unsat. Hard Rock</b>		2.4	3.2	2.81	824	2700	2.22e+06
<b>Crystalline</b>				3.00	790	2750	2.17e+06
Source: see Hardin et al. 2012b for details.							

Additional properties are discussed in Sections 2, 3 and 4. Creep and thermal properties for salt, and their temperature dependence are discussed in Section 3. Thermal-hydrologic properties of the backfill and host formation are discussed in Section 4.

Table 1-5. Repository dimensions and other concept data for generic host media.

Repository Depth	Approx. Drift Dimensions	Package Placement	Drift Spacing <sup>A</sup>	Package Spacing <sup>A</sup>	Backfill	WP Emplacement Power Limit	Areal Power	Repository Layout Area
<b>Salt</b>								
500 to 1,000m	4m H x 6m W	Directly on floor <sup>D</sup>	30m	30m	Crushed salt	10kW	11 W/m <sup>2</sup>	~15 km <sup>2</sup>
<b>Clay/Shale</b>								
500m	4.5m H x 4.5m W mailbox <sup>B</sup>	Directly on floor	70m	20m	Crushed shale/dehydrated swelling clay mixture	4kW	3 W/m <sup>2</sup>	~40 km <sup>2</sup>
<b>Unsaturated Alluvium</b>								
>200m	4.5m H x 4.5m W mailbox <sup>B</sup>	Directly on floor	70m	20m	Crushed/sorted alluvium	4kW	3 W/m <sup>2</sup>	~40 km <sup>2</sup>
<b>Unsaturated Hard Rock</b>								
>200m	4.5m H x 4.5m W mailbox <sup>B</sup>	Directly on floor	81m	5m	Crushed/sorted rock	11.8kW max.; 1.45 kW/m avg.	17 W/m <sup>2</sup>	~5 km <sup>2</sup>
<b>Crystalline</b>								
500m	4.5m dia. circular	Centered within a clay buffer	50m	20m	Dehydrated swelling clay	3 kW <sup>C</sup>	3 W/m <sup>2</sup>	~15 km <sup>2</sup>
<sup>A</sup> Spacings are center-center. <sup>B</sup> Mailbox has 4.5m dia. semi-circular roof; cross-sectional area equivalent to 4.8m dia. circular opening. <sup>C</sup> A package power limit of 2 kW could be required to limit peak buffer temperature to 100°C. <sup>D</sup> May be placed into a semi-cylindrical cavity in the floor to provide mechanical support to the overpack, and improve heat transfer (SNL 2019). Source: SNL 2020. <i>DPC Disposal Concepts of Operations</i> . M3SF-20SN010305052 Rev. 0.								



## 2. Semi-Analytical Model

The semi-analytical method is based on the approach developed in FY11 specifically for enclosed emplacement modes to investigate waste inventory, geologic setting, and operations (Figure 2-1; see Hardin et al. 2011). The MathCad script was later modified to investigate open modes and the associated effects from ventilation, backfill, package size, etc. (Hardin 2013).

This study models enclosed reference repository concepts for DPC-based waste packages (SNL 2020) with as-loaded DPC thermal power histories described in Section 1.

Thermal responses for these waste forms were investigated for reference disposal concepts in several generic host media (unsaturated hard rock, clay/shale, alluvium, bedded salt, and crystalline basement rock for deep borehole emplacement). The thermal analysis presented here calculates: 1) temperature history at or near the interface between the backfill and the host medium (drift wall); and 2) temperature history at the surface of the waste package overpack. For the drift wall the temperature history is estimated by superposing analytical, Fourier conduction solutions for a finite line source (representing a central package), point sources (adjacent packages in the same drift or alignment), and line sources (adjacent drifts or alignments). The approach is described elsewhere (Hardin et al. 2012, Section 3 and Appendix A).

The forcing function for all sources is a transient time series representing the decaying waste. A transient superposition solution (temperature vs. time) is generated for a point on the perpendicular mid-plane for the central package, at a distance corresponding to the drift wall (Figure 2-1). Temperatures for annular layers representing the engineered barrier system (EBS; i.e., backfill, buffer, air gap, etc.) within that distance are then calculated using a steady state solution. Temperature is slowly varying, and the sensible heat stored within that distance is very small compared to the overall heat output of the waste. For air gaps in the unsaturated hard rock case, a gray-body, thermal radiation solution for concentric surfaces is used.

For this report the EBS is limited to the backfill or air gap (unsaturated hard rock case), and the waste package which includes a hypothetical 7 cm thick overpack. Actual overpack designs would be site and geologic medium specific and are beyond the scope of this report. Thermal histories are presented for each as-loaded DPC of interest labeled by their percentile of thermal output: 99<sup>th</sup>, 95<sup>th</sup>, 90<sup>th</sup>, 75<sup>th</sup>, 50<sup>th</sup> and 10<sup>th</sup>. The central finite line source uses the decay profile from the percentile of interest and the far field infinite line and point sources use the 75<sup>th</sup> percentile profile. Repository dimensions are shown in Table 1-5, and thermal properties are presented in Section 1.

The unsaturated hard rock case is unbackfilled and the waste package is thermally coupled to the drift wall by thermal radiation, with emissivity values of 0.8 and 0.9 for the waste package and drift wall, respectively. For all but the salt case, the backfill/buffer material is assumed to be clay-based with a thermal conductivity of 1.5 W/m-K.

Because the thermal conductivity of crushed salt backfill begins at several times less than for intact salt, but material the consolidates over time, an estimated backfill thermal conductivity appropriate for calculating peak temperature is used. Heat-generating waste packages would be placed into semi-cylindrical cavities milled in the alcove floor to improve heat transfer to the intact salt where at least half of the waste package circumference is in close contact with intact salt. The thermal conductivity used is taken as the thermal conductivity of intact salt at 200°C, but with only 75% of the periphery available to transfer heat.

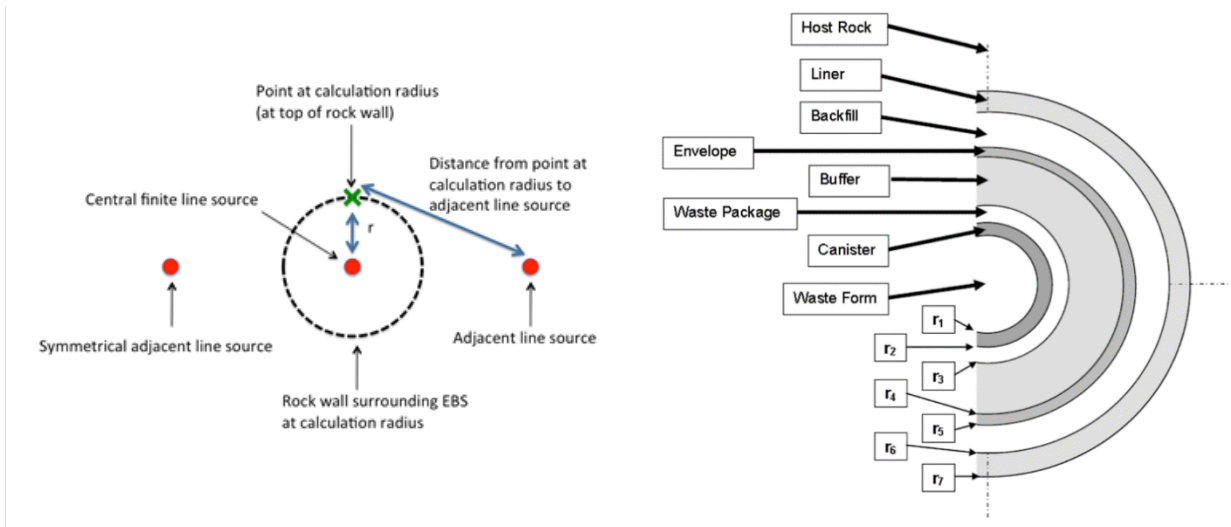
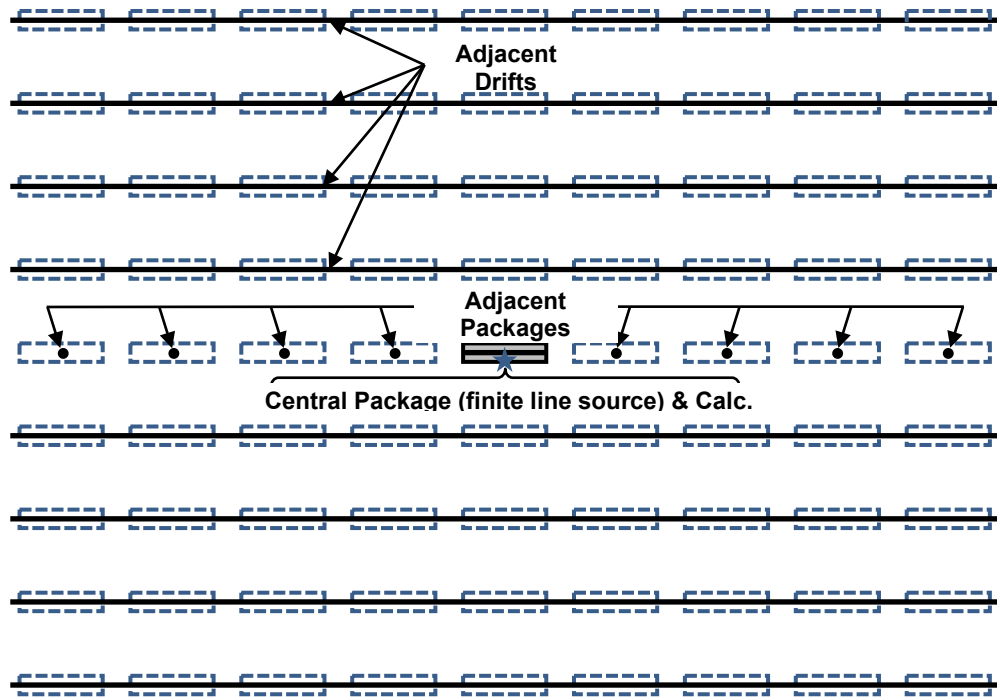


Figure 2-1. Schematic of semi-analytical model elements superimposed.

Table 2-1. Geometry and near-field properties for semi-analytical model.

Concept	Drift Radius (m)	Drift Spacing (m)	Package Spacing (m)	Backfill $K_{th}$ (W/m-K)	Package Emissivity	Wall Emissivity
Unsaturated Hard Rock	2.4	81	5	–	0.6	0.9
Clay/Shale	2.4	70	20	1.5	–	–
Alluvium	2.4	70	10	1.5	–	–
Salt	2.76	30	30	3.21 ( $\times 0.75$ )	–	–
Crystalline	2.25	50	20	1.5	–	–

The analytical solutions are coded using MathCad Prime 5<sup>®</sup>. This script offers five disposal concepts (“Rock\_type”) each with specified geometry and properties. The realistic DPC (“WF\_name”) thermal histories, number of assemblies loaded in the canister (“WF\_cnt”), and package dimensions (“Assy\_layer\_inner\_r” and “WP\_len”) are specified for each DPC.

## 2.1 Results Summary

Peak drift wall temperature and peak waste package overpack surface temperature are tabulated in Table 2-2 for each heat output percentile and each geologic medium. The time at which the peak occurs is shown in terms of the calendar year assuming emplacement at calendar 2100.

Table 2-2. Results summary for percentiles of heat output and different disposal concepts using wet thermal conductivities.

WP Percentile	Alluvium				Clay/Shale				Crystalline			
	Peak WP T (°C)	Time of Peak (Cal yr)	Peak Wall T (°C)	Time of Peak (Cal yr)	Peak WP T (°C)	Time of Peak (Cal yr)	Peak Wall T (°C)	Time of Peak (Cal yr)	Peak WP T (°C)	Time of Peak (Cal yr)	Peak Wall T (°C)	Time of Peak (Cal yr)
10th	202	2417	181	2487	121	2137	90	2427	114	2218	89	2395
50th	238	2131	191	2447	169	2113	102	2198	145	2122	95	2336
75th	267	2120	197	2417	199	2110	111	2136	168	2111	99	2306
90th	297	2116	203	2344	260	2107	128	2122	191	2108	103	2259
95th	311	2114	209	2136	242	2107	132	2118	201	2106	104	2203
99th	362	2112	228	2130	291	2107	150	2117	241	2105	113	2146

WP Percentile	Unsat. Hard Rock				Salt			
	Peak WP T (°C)	Time of Peak (Cal yr)	Peak Wall T (°C)	Time of Peak (Cal yr)	Peak WP T (°C)	Time of Peak (Cal yr)	Peak Wall T (°C)	Time of Peak (Cal yr)
10th	177	2544	175	2559	107	2213	85	2306
50th	183	2502	180	2521	129	2153	90	2273
75th	186	2481	182	2503	144	2128	93	2257
90th	189	2439	185	2481	161	2118	96	2237
95th	191	2117	186	2481	169	2112	97	2221
99th	203	2116	192	2118	199	2109	103	2197

The effect of buffer dryout has a significant impact on waste package temperature which increases as the power level of the DPC increases as shown in Figures 2-2 and 2-3, for the 10<sup>th</sup> and 50<sup>th</sup> percentile of heat output, respectively. These selections represent what might be achieved with additional aging of hotter DPCs. The effect from buffer dryout is more pronounced soon after emplacement when peak temperature occurs, which suggests that a backfill/buffer additive is needed to increase thermal conductivity.

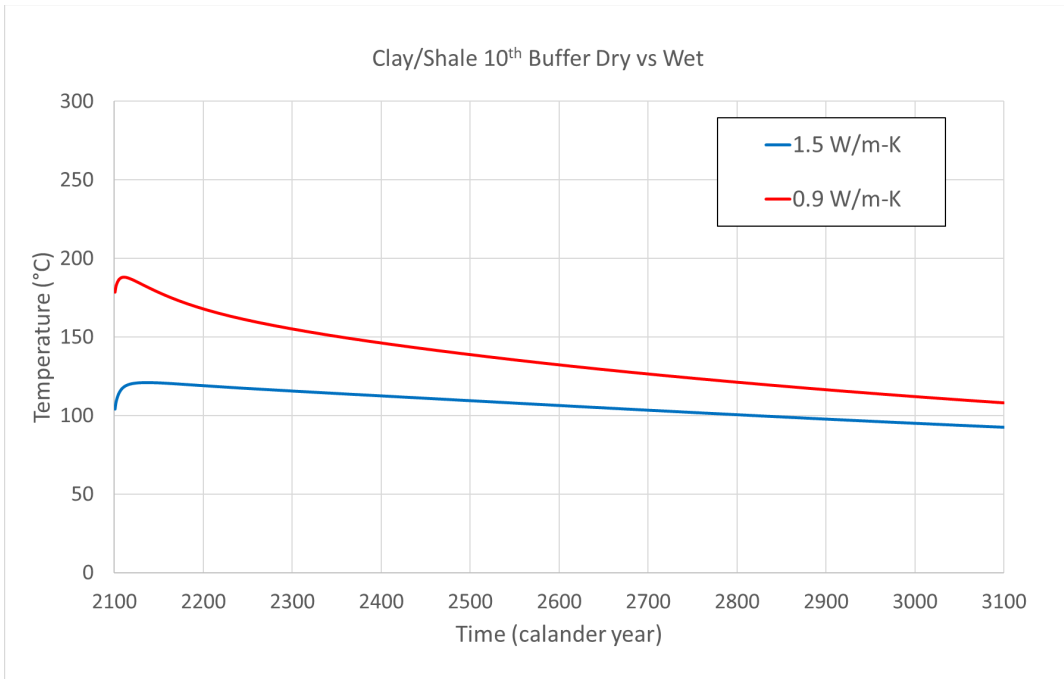


Figure 2-2. Comparison of waste package overpack surface temperature histories with dry and wet backfill/buffer, for the clay/shale repository concept with 10<sup>th</sup> percentile heating.

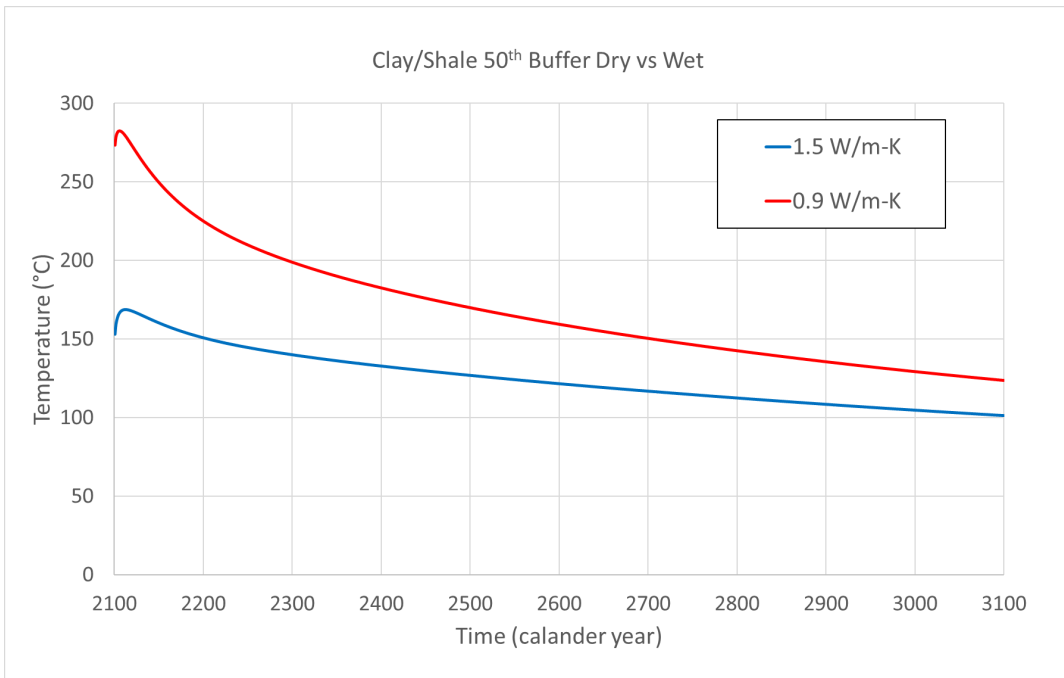


Figure 2-3. Comparison of waste package overpack surface temperature histories with dry and wet backfill/buffer, for the clay/shale repository concept with 50<sup>th</sup> percentile heating.

### 3. Thermal Creep Model for a Salt Repository

FLAC V7.0 (Itasca 2011) was used for 2-D plane-strain simulation of a waste package surrounded by crushed salt, within a rectangular tunnel opening (Table 1-5). The constitutive laws for crushed and intact salt were *cwipp* and *pwipp*, respectively, which are built-in FLAC viscoplastic models based on an early creep law (Senseny 1985). As discussed below, the choice of creep laws is not critical to this study because backfill consolidation always occurs.

Modeling studies were done in 2D to investigate how creep and temperature-dependent  $K_{th}$  affect temperature evolution, and the range of peak near-field temperatures that can be expected in a salt repository for DPC-based waste packages. A 3D approach would likely be used in the future to support repository conceptual design, using site specific thermal and mechanical salt properties.

The application requires coupling between temperature and thermal conductivity, and between creep strain and thermal conductivity. Both couplings are two-way because thermal conductivity affects both temperature and creep rate in the model. Coupling of  $K_{th}$  to temperature is performed using an intrinsic function of FLAC as discussed below. Coupling of  $K_{th}$  to crushed salt porosity (intact salt always has zero porosity in this model) is accomplished with periodic updates implemented using the FISH scripting language within FLAC. The update interval varies between 0.05 yr and 10 yr in models that run to 300 yr duration, with shorter intervals used in the first few years and decades while creep consolidation of the backfill is active.

#### Model Inputs

Thermal conductivity ( $K_{th}$ ) of crushed salt backfill is a function of both porosity and temperature, whereas the intact salt  $K_{th}$  is a function of temperature only because its porosity is always zero (or nearly so). The temperature dependence is the same function for salt backfill and intact salt, and the backfill  $K_{th}$  is determined by scaling the temperature-dependent result.

The temperature effect on  $K_{th}$  was incorporated using an intrinsic FLAC function (*th\_general*) so that  $K_{th}$  updates for temperature changes were made without interrupting time stepping. The *th\_general* function of the form

$$K_{th} = C_1 + C_2 (300/T)^\lambda \quad (3-1)$$

was fitted to the Bechthold et al. (2004)  $K_{th}(T)$  function (Figure 3-1),

$$K_{th} = 5.734 - 0.01838 T + 0.0000286 T^2 - 1.51 \times 10^{-8} T^3 \quad (3-2)$$

A specific heat value of 900 J/kg-K was selected based on similar values reported by Bechthold et al. (2004) for both intact and crushed salt.

Porosity dependence for the crushed salt backfill was represented using a polynomial fit to field test data (Bechthold et al. 2004):

$$K_{crushed}(\varphi) = -270 \varphi^4 + 370 \varphi^3 - 136 \varphi^2 + 1.5 \varphi + 5 \quad (3-3)$$

which is reported to be valid for porosity  $\varphi$  up to 40%. The polynomial yields 5.0 W/m-K at zero porosity, but it can be scaled by a factor, to represent similar values. For this study it was scaled to 5.4 W/m-K (the temperature dependence  $K_{th}$  value at a temperature of 300 K).

Salt thermal expansivity of  $13.83 \times 10^{-5}/K$  (volumetric) was obtained from Robinson (1988, Table 9, halite). The coefficient of linear thermal expansion is one third of this value. The

corresponding reported density value is  $2.163 \text{ Mg/m}^3$ , which is about 3% larger than the value of  $2.100 \text{ Mg/m}^3$  used in this study.

Creep properties were taken from Itasca (2011) for the *pwipp* and *cwipp* models; these property values are attributed to Senseny (1985). Initial backfill porosity was set to 36%, consistent with estimates for porosity of granular materials. This value is the minimum reported porosity for a closest packing of uniform spheres. Similar in situ porosity values for crushed salt (35% to 38%) were reported by Bechthold et al. (2004).

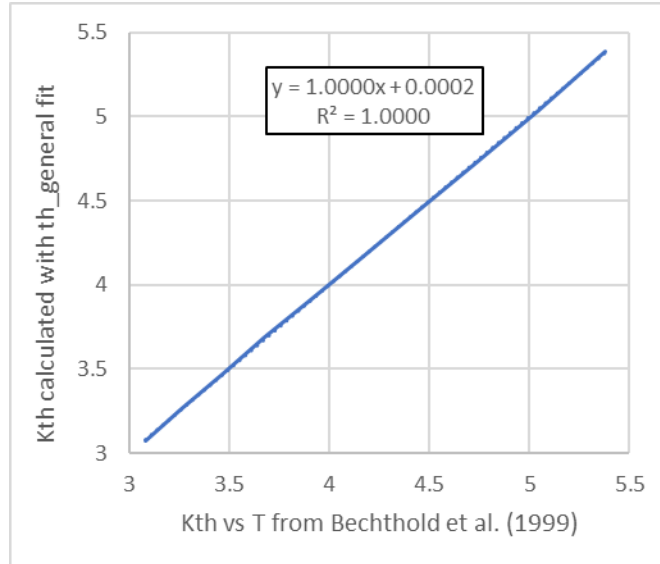


Figure 3-1. Cross-plot between  $K_{th}$  values (functions of temperature) calculated using the fit from Bechthold et al. (2004), and the intrinsic FLAC *th\_general* function.

### 3.1 Reference Case

This section discusses a reference case (Figures 3-2 and 3-3) which uses a 1-m grid, 99<sup>th</sup> percentile heating, unmodified *pwipp* and *cwipp* creep parameters, temperature dependent  $K_{th}$ , and backfill porosity-dependent  $K_{th}$ . The line-load heating rate is scaled to represent packages spaced 10 m apart center-center (this approximation is addressed further in Section 3.5). Peak temperatures at the drift wall are in the range 410 to 430 K (137 to 157 C), and occur at approximately 150 yr (calendar 2250). Peak magnitude and timing are discussed further in Section 3.2. Sawtooth behavior of temperature, evident in many of the plots in this section, results from periodic updates of backfill  $K_{th}$  and disappears after the backfill consolidates.

The FLAC code uses fully explicit Eulerian finite difference time stepping for both mechanical deformation and heat transport. The sizes of time steps can be determined automatically based on stability criteria, or they can be specified along with the number of steps to be executed. For coupled mechanical-thermal problems it is desirable to synchronize “creep time” with “thermal time” so as to avoid conflicts. For this reason, the approach used here is to specify equivalent mechanical and thermal time steps, and synchronize. Some trial-and-error is needed with this approach to determine time step values and backfill  $K_{th}$  update intervals of appropriate sizes to avoid numerical instability.

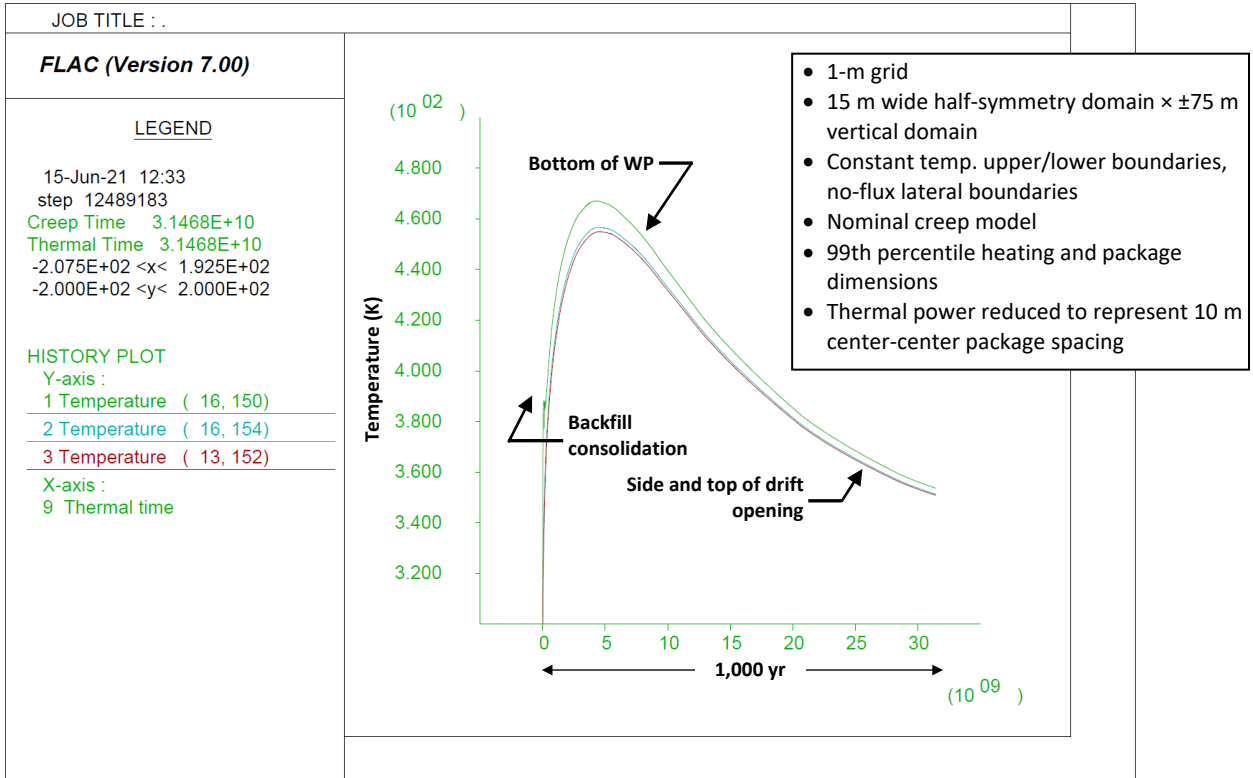


Figure 3-2. Reference case temperature histories at three locations on the drift wall, as noted.

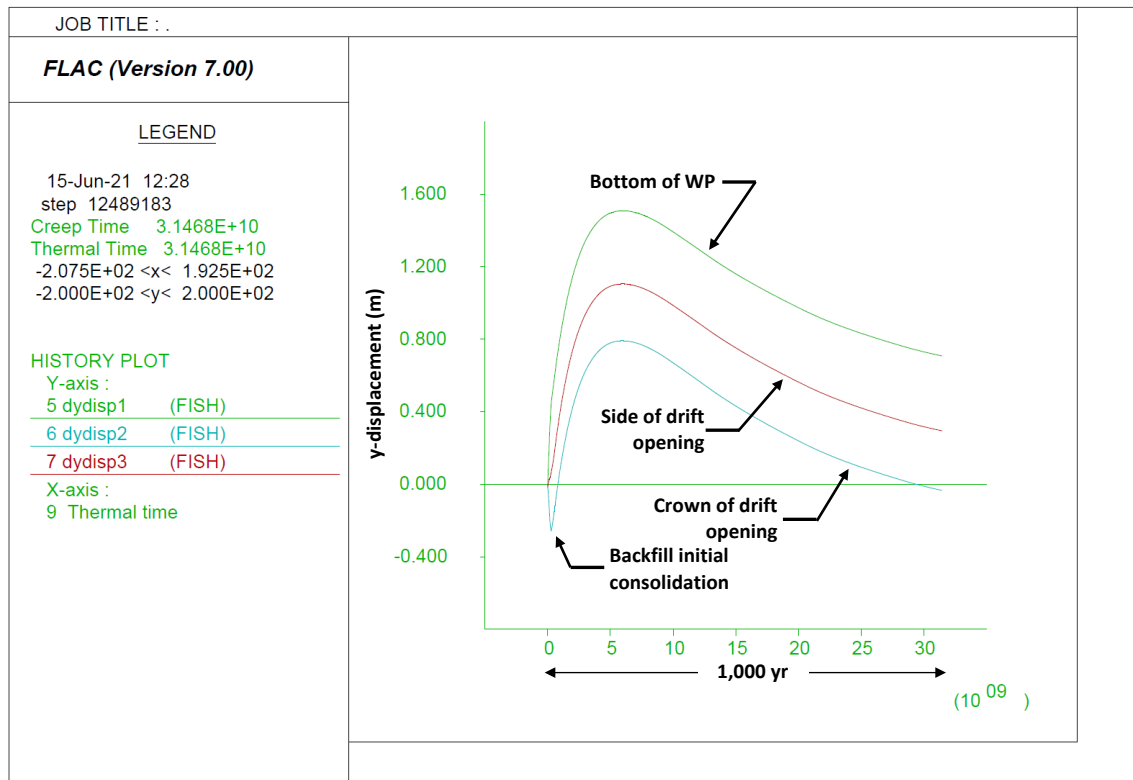


Figure 3-3. Reference case y-displacement histories at three locations on the drift wall, as noted.

Damping is in effect at the beginning of each run, attenuating the oscillation of displacements (amplitude of order 1 cm) within a few days or weeks of simulation time. This response can be further attenuated by increasing the FLAC damping parameter, but with potential effects on accuracy of calculated displacements.

Damped oscillation of temperature also occurs after a very small portion of backfill property updates (less than 1%) which can be seen in several of the temperature history plots in the following sections. The most effective measures to eliminate these excursions are to use small update intervals (typically  $\ll 1$  yr) and to increase the thermal and mechanical time steps just prior to the occurrence. However, this may be only partially successful if oscillations then occur somewhere else in the run history. These unwanted excursions occur only for coupled thermal-creep problems, and not for creep-only or thermal-only runs.

The temperature curve for the point at the center-bottom of the waste package exhibits an initial rise prior to backfill consolidation, then a decrease after consolidation approaches completion (Figure 3-2). This transient lasts tens of years and is the main thermal effect from creep. It can be seen more clearly in other plots discussed below. No other oscillatory behavior is evident in these reference case figures.

Displacement curves (Figure 3-3) are plotted from the onset of heating (they do not include the initial elastic gravitational equilibration of the model). These y-displacement curves combine two responses: initial creep closure of the drift opening for approximately 100 to 200 years, and thermal expansion of the entire model resulting in upward displacement followed by cooling and downward displacement. In Figure 3-3 the creep closure response dominates thermal expansion.

### **Thermal Creep vs. Thermal-Only Study**

The influence of creep consolidation of backfill on temperature histories is shown by comparison of Figure 3-4 (reference case with creep, but with  $\pm 150$  m vertical domain) and Figure 3-5 (no mechanical deformation, although  $K_{th}$  does vary with temperature). The effect of creep is to delay the peak temperature beneath the waste package, while temperatures elsewhere on the drift wall occur at approximately the same times as for the no-creep case.

Peak temperature magnitude at the drift wall is slightly higher for the creep case, since consolidated backfill conducts more heat to these locations. The difference is small, on the order of 10 K. At the drift wall location under the waste package, peak temperature is greater (about 25 K) because without backfill consolidation, more heat is forced into the intact salt beneath the package.

### **Activation Energy (Creep Rate) Study**

The *pwipp* and *cwipp* creep models use an Arrhenius expression to represent thermal activation. The creep strain rate is multiplied by a factor:

$$\dot{\epsilon} \propto \exp\left(\frac{-E_A}{RT}\right) \quad (3-4)$$

where  $E_A$  is the activation energy (cal/mol),  $R$  is the universal gas constant (1.987 cal/mol-K), and  $T$  is absolute temperature (K). For this study,  $E_A$  was increased to study the impact on temperature predictions, from uncertainty in backfill consolidation rate (and creep closure of the intact salt). The activation energies for both the intact and crushed salt were increased by 20% and 30% (Figures 3-6 and 3-7) for comparison to the base case *pwipp* and *cwipp* models (Figure 3-4).



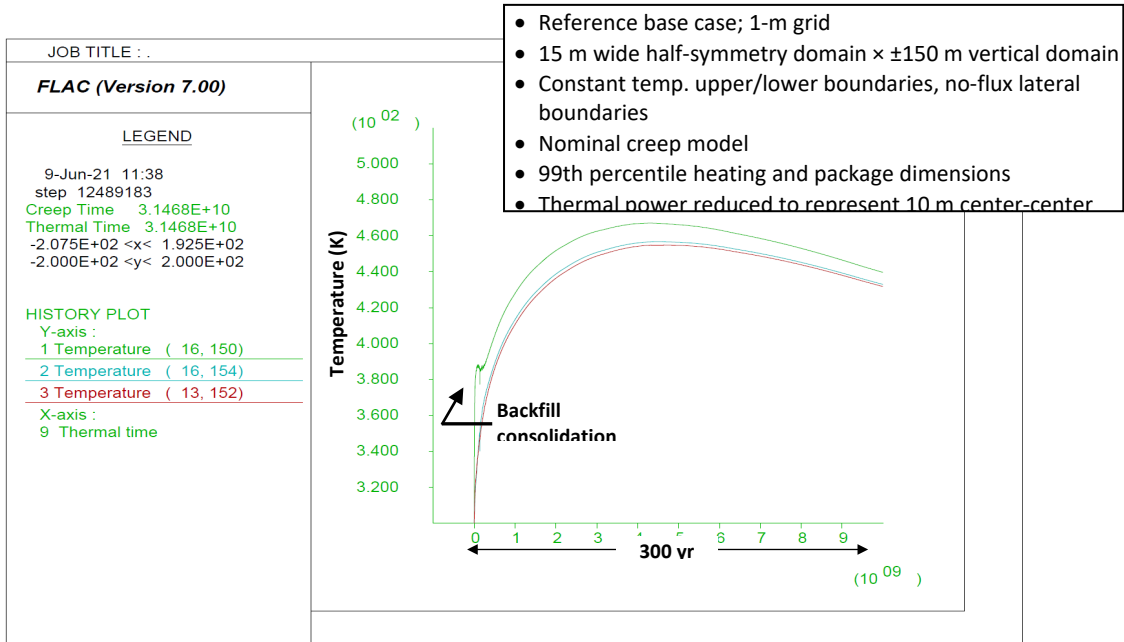


Figure 3-4. Reference case temperature histories (similar to Figure 3-2 but greater vertical extent).

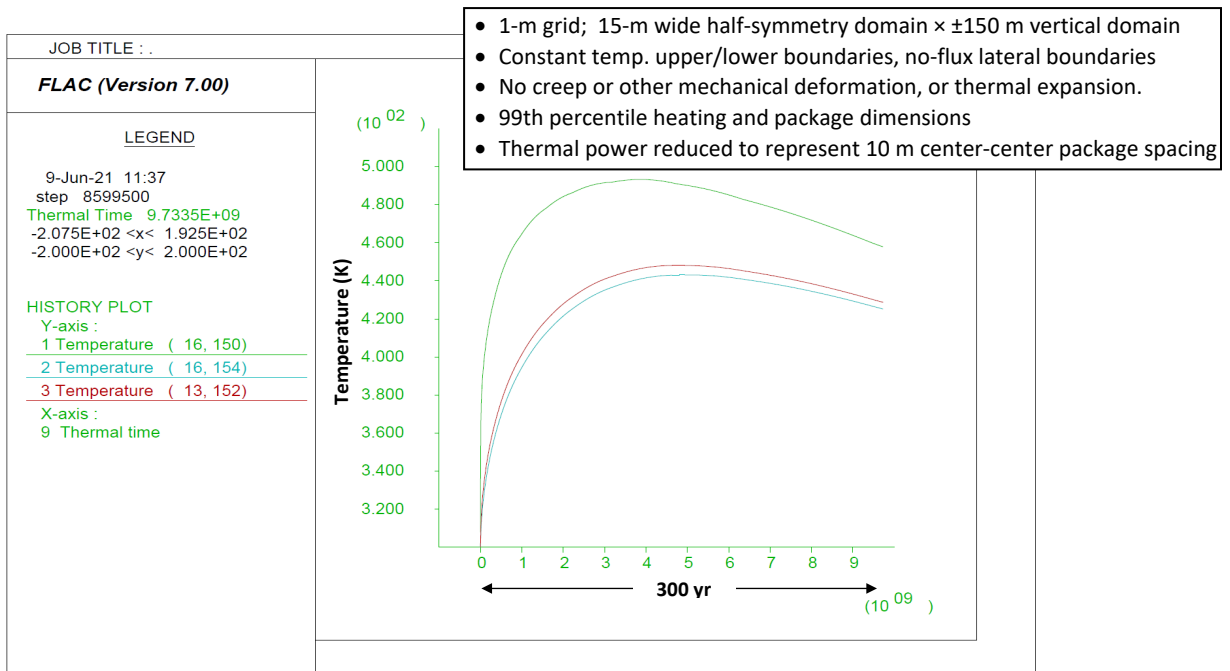


Figure 3-5. Temperature histories with creep turned off, and  $K_{th}$  dependent on temperature. Compare to Figure 3-4.

With the creep rates slowed down there is: 1) faster initial temperature rise in the wall temperature under the waste package (and in the package temperature as well) as shown in Figures 3-6 and 3-7; and 2) suppression of temperature rise at other locations on the drift wall since backfill

consolidation is delayed keeping  $K_{th}$  low. If creep rates are slowed enough, then the initial rise produces the peak temperature overall (Figure 3-7), at an earlier time on the order of 30 yr.

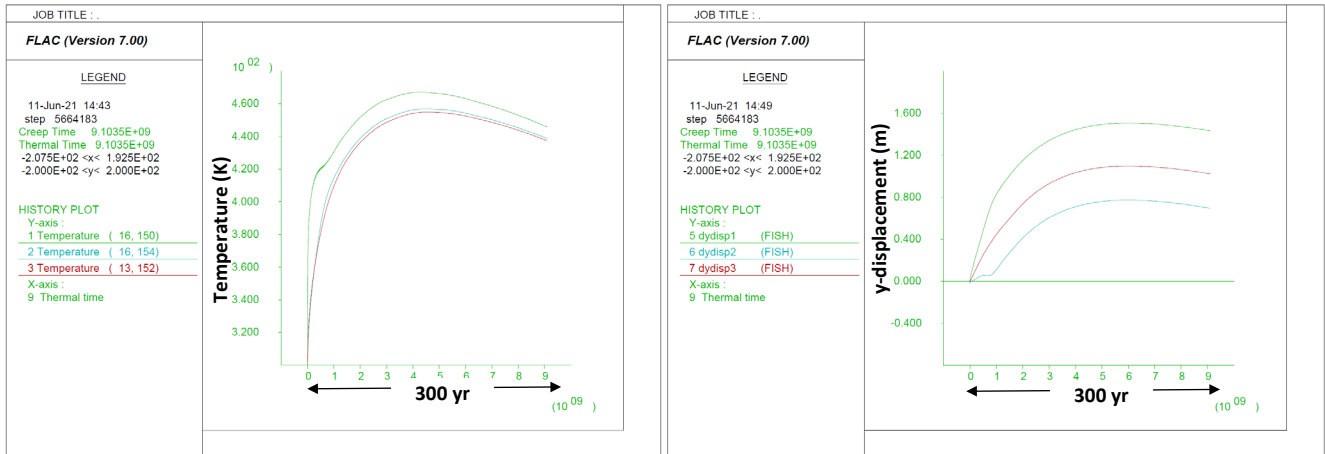


Figure 3-6. Histories of drift wall temperature (left) and displacements (right) with  $E_A$  increased 20% (creep rate multiplier 0.034 at 373 K, 0.069 at 473 K). Compare to Figure 3-4.

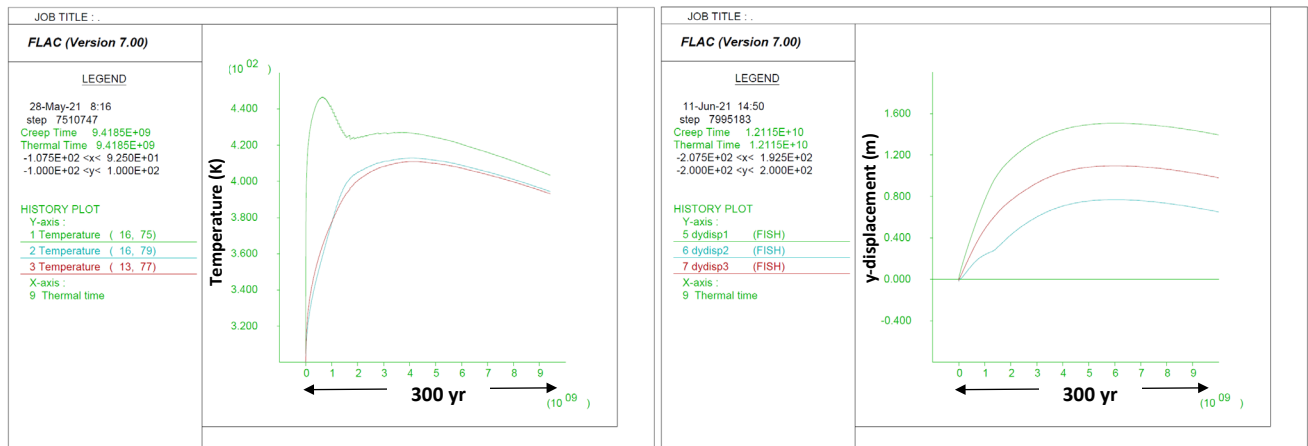


Figure 3-7. Histories of drift wall temperature (left) and displacements (right) with  $E_A$  increased 30% (creep rate multiplier 0.0062 at 373 K, 0.018 at 473 K). Compare to Figure 3-4.

This exercise has shown that backfill creep consolidation rate has a small effect on peak near-field temperatures that occur beyond about 100 years, except if the rate is slowed by more than an order of magnitude from the nominal *cwipp* rate. Hence, the models used to represent creep of intact and crushed salt may be of secondary importance to other uncertainties such as the effect of elevated temperature on  $K_{th}$ , and the final fractional density of crushed salt (may be less than 1).

### 3.2 Grid Size and Resolution Studies

Grid size was addressed by comparing runs similar to the reference case described above, with vertical domain height  $\pm 75$  m and  $\pm 150$  m. The results were interpreted using the well-known relationship for thermal diffusion:

$$\frac{L^2}{\alpha} \propto t \quad (3-5)$$

where  $L$  is distance,  $t$  is characteristic time, and  $\alpha$  is thermal diffusivity. Diffusivity is estimated to be  $2.64 \times 10^{-6}$  m<sup>2</sup>/sec ( $K_{th} = 5$  W/m-K, density 2,100 kg/m<sup>3</sup>, and specific heat 900 J/kg-K). With  $L$  set to 75 m or 150 m, the characteristic time is 67 yr or 270 yr, respectively. Peak temperature as the principal metric of thermal management, and peak near-field temperatures in a salt repository apparently occur at less than 300 yr after emplacement, so the  $\pm 150$  m vertical domain is a reasonable choice. Recommended future work using alternative software and/or more refined grids may show that a greater vertical domain is needed. The timing of peak near-field temperature is discussed further below.

Grid resolution was investigated by running similar cases with grid size of 1 m, 0.5 m, and 0.25 m (Figure 3-8). The cases were thermal-only models with no creep, which expedited the calculations and narrowed the resolution study to thermal modeling. The cases used 99<sup>th</sup> percentile heating,  $K_{th}$  of 5 W/m-K for intact salt (fixed with respect to temperature), and 1 W/m-K for crushed salt (also fixed). The latter value is reduced somewhat and similar to values obtained for crushed salt in the first few decades after emplacement.

The grid resolution study (Figure 3-8) shows the apparent interplay of numerical diffusion and the constant temperature upper and lower model boundaries. Numerical diffusion lowers peak near-field temperatures due to faster transport of heat to the far field. However, numerical diffusion also increases the effective  $\alpha$  in Eqn. 3-5, which slightly accelerates and increases the amplitude of peak suppression from the constant temperature boundaries. Consistent with this explanation, the 1-m grid produced a somewhat slower rise in near-field temperatures than the 0.5-m and 0.25-m grids, and smaller peak temperature than the 0.5-m case (peak of about 430 K vs. 480 K for the finer grid). The 0.25-m grid produced the fastest early rise in temperature (especially at the base of the waste package).

Hence, the 1-m grid may be under-predicting temperature compared to the 0.5-m grid. However, the 0.25-m grid produced near-field peak temperatures smaller than the 0.5-m grid, and closer to the 1-m grid. Peak temperatures in the 0.25-m case took roughly twice as long as the other cases (e.g., 350 yr vs. 150 yr) possibly because the numerical diffusion effect was smaller. This trend should be investigated by extending the upper and lower model boundaries much further away (e.g., 500 m), which might be accomplished efficiently using a nested grid strategy.

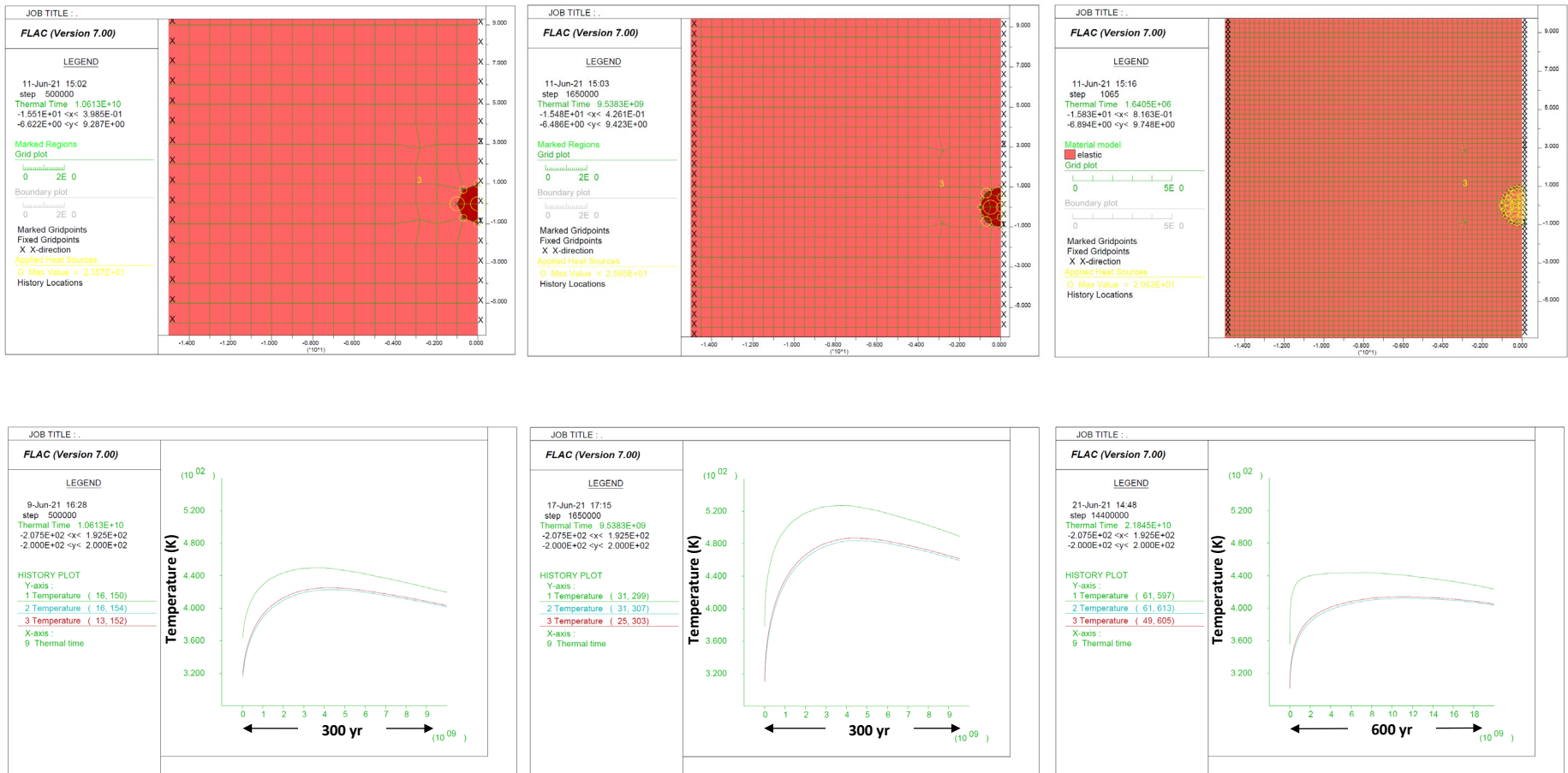


Figure 3-8. Grid resolution study comparing drift-wall temperatures (lower) for grid resolution of 1 m, 0.5 m, and 0.25 m (upper, excerpted from the larger  $\pm 150$  m model grids). Temperature histories for 300 yr are shown in the lower plots, for grid resolution of 1 m, 0.5 m, and 0.25 m (left to right). Cases were run using 99<sup>th</sup> percentile heating, fixed intact salt and backfill  $K_{th}$ , and no creep.

### 3.3 Comparison of FLAC 2D Model with Semi-Analytical 3D Model, Peak Temperature

The FLAC thermal-creep model is useful for describing the early-time near-field temperature response associated with creep consolidation of crushed salt backfill. The semi-analytical model (Section 2) is most useful for describing temperature evolution from the drift wall outward, with a concentric circular geometry of the drift opening and waste package. Comparison of the two approaches is done two ways: 1) using a benchmark which is a simplified line-load case; and 2) adjusting the equivalent package spacing parameter in the FLAC model to match drift-wall peak temperature from the semi-analytical (MathCad) model.

#### Benchmark

For the benchmark case the  $K_{th}$  for both intact salt and backfill is set to a constant value of 5.0 W/m-K, and the porosity of both is set to zero (2,100 kg/m<sup>3</sup> density). The principal differences between the models are the presence of constant-temperature upper and lower boundaries, eccentric waste package geometry, and rectangular drift opening shape in the FLAC model. By contrast, the semi-analytical model is embedded in an infinite space, with concentric waste package geometry, and a circular drift opening. For both models, 99<sup>th</sup> percentile heating is used with image sources or reflecting boundaries representing an infinite array of packages.

The results are comparable in terms of peak temperature magnitude and timing (Figure 3-9). The semi-analytical model calculates peak temperature of approximately 600 K, occurring during an interval from about  $3.5 \times 10^9$  to  $5 \times 10^9$  sec (110 to 160 yr). The FLAC model calculates a peak temperature of approximately 565 K, occurring at about  $4.5 \times 10^9$  sec (140 yr). The FLAC temperature is lower, probably due to the onset of cooling from the constant temperature upper and lower boundaries, and due to numerical diffusion occurring with larger grid blocks, as shown in Section 3.2.

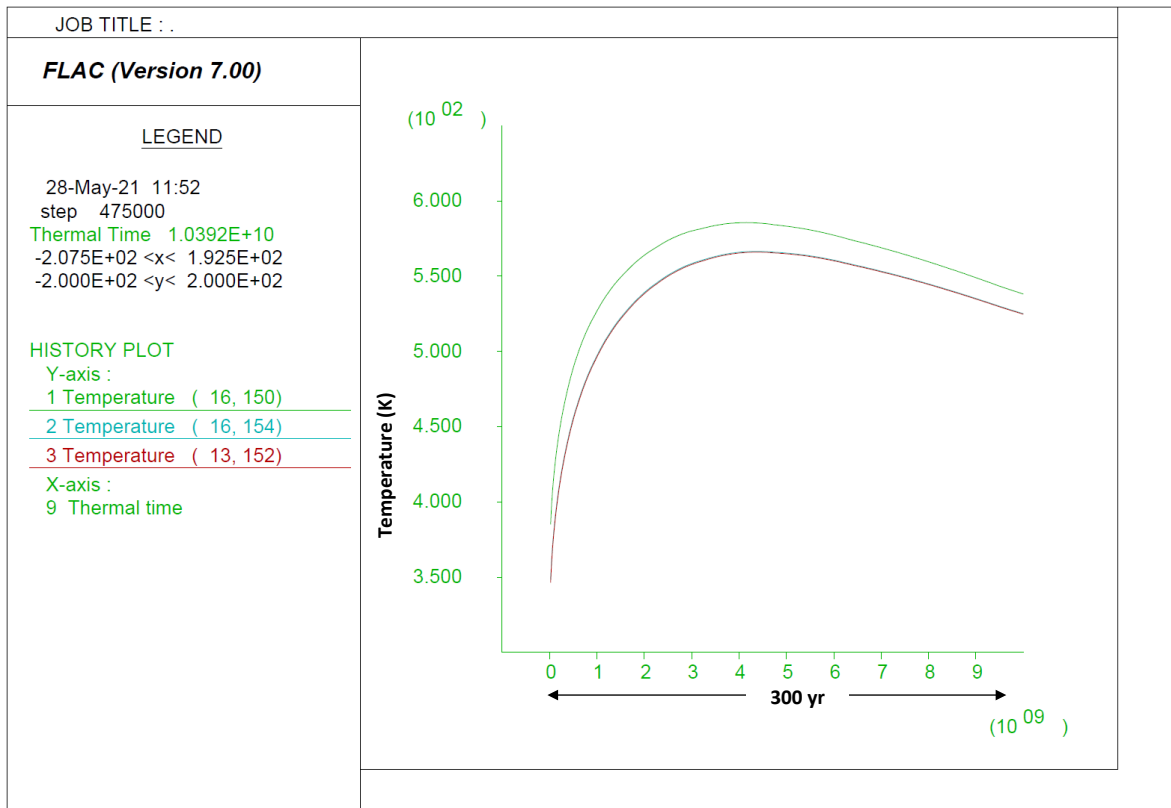
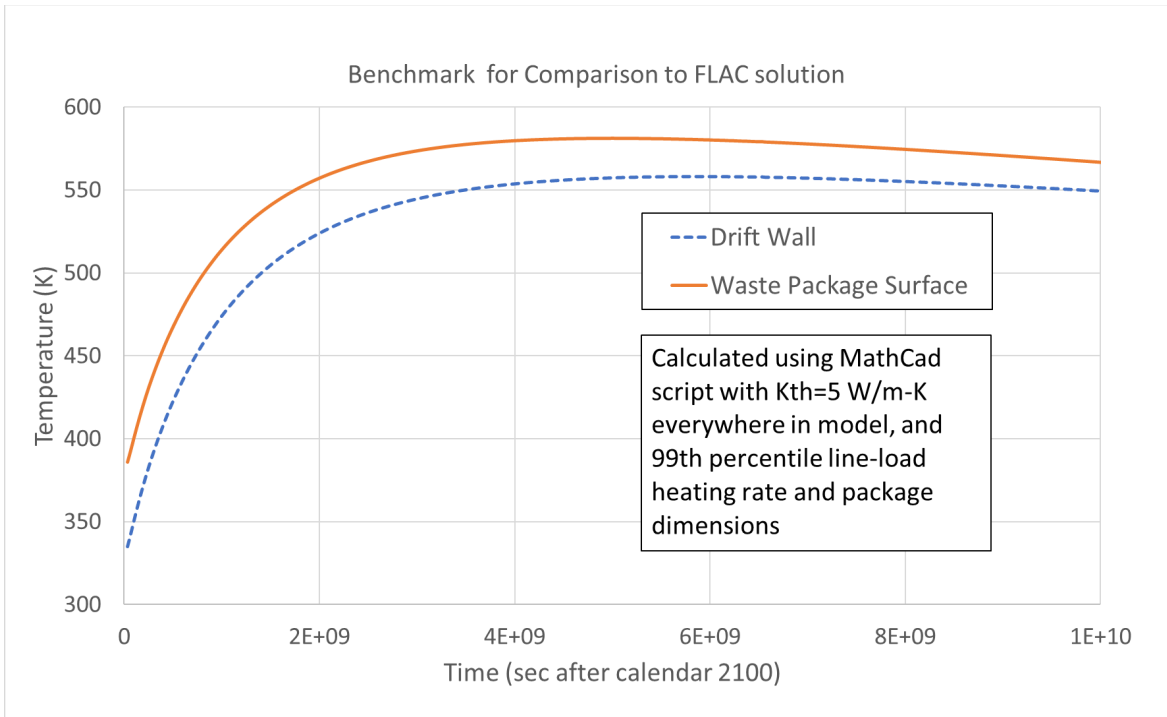


Figure 3-9. Benchmark line-source runs with the semi-analytical model implemented in MathCad (upper), and a similar 2D FLAC model (lower).

### 3.4 “Calibration” of the 2D Line Source to Match 3D Peak Temperature at the Drift Wall

This section evaluates the fidelity of the 2D line-source implemented in the FLAC model, with the 3D point-loading scheme implemented in the semi-analytical model, for SNF emplacement in salt. The point of comparison is at drift wall, adjacent to the waste package mid-point, where it is maximal. The line-load strength in the FLAC model is adjusted between a true line load (package spacing equal to package length, or 4.974 m for the 75<sup>th</sup> percentile case), and the associated point load (package spacing 30 m). The FLAC model was run with this spacing parameter set to 4.974, 10, 20 and 30 m, for comparison to a point-load calculation with the semi-analytical model with 30-m spacing. The FLAC runs scale linearly to the source strength, so the temperature rise (above the initial temperature of 300 K) scales linearly to the reciprocal of this spacing parameter.

To simplify the runs and focus on geometry of heat transport (assuming perturbation of heat flow from creep consolidation of backfill is short-lived), the  $K_{th}$  for intact salt was fixed at 5 W/m-K, and  $K_{th}$  of the backfill was fixed at 1 W/m-K. All the runs used 75<sup>th</sup> percentile heating. The FLAC runs set the upper and lower boundaries at  $\pm 150$  m, with grid resolution of 1 m. The peak temperature results are tabulated in Table 3-1.

Table 3-1. Summary of 2D line-load “calibration” exercise.

Run	Spacing (m)	Peak Temp. (K)	Time of Peak (sec)
PS4.974m	4.974	545	4.9e9
PS10m	10	422	4.9e9
PS20m	20	361	4.9e9
PS30m	30	341	4.9e9
Semi-analytical (MathCad)	30	345	3.4e9

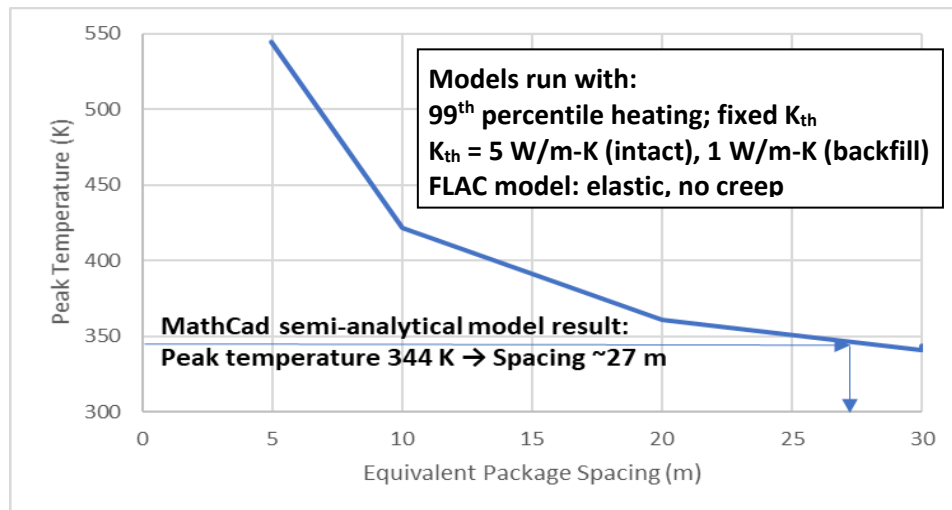


Figure 3-10. “Calibration” of 2D FLAC line-load thermal model to 3D semi-analytical model implemented in MathCad.

Plotting the FLAC results and comparing to the semi-analytical result shows that the equivalent spacing parameter is approximately 27 m (Figure 3-10), close to the true spacing of 30 m. This suggests that 2D models can be used to estimate 3D point-loading peak temperatures, although the 2D approximation is likely to underestimate temperature near the waste package mid-point, and overestimate temperature between packages.

### 3.5 Temperature and Displacement Histories for Percentile DPCs

Temperature and y-displacement histories are presented for the 99<sup>th</sup>, 90<sup>th</sup>, 50<sup>th</sup>, and 10<sup>th</sup> percentile heating data, using the reference (*pwipp* and *cwipp*) creep models and thermal properties as discussed above (Figures 3-11 and 3.12). These results were calculated using the 1-m grid, with boundaries  $\pm 150$  m above and below the waste package. The heating function was attenuated, multiplied by the ratio of waste package length to the “calibrated” 27-m center-center package spacing from Section 3.4.

Temperature histories are similar although the lower percentiles are scaled to lower temperatures, as expected. The displacement histories have two parts: 1) an early shift due to backfill consolidation, particularly at the drift wall directly above the waste package; and 2) a longer-term trend associated with thermal expansion of the far field that lifts the entire model upward toward the free surface. The thermally activated backfill creep consolidation response is slower in the cooler cases (50<sup>th</sup> and 10<sup>th</sup>) because temperatures are lower. The longer-term trend is similar in all cases, although smaller in the cooler cases.

Importantly, even the 99<sup>th</sup> percentile case with backfill consolidation and temperature-dependent  $K_{th}$ , and “calibration” to the 3D semi-analytical solution, produces peak drift-wall temperatures on the order of 350 K (80°C). For comparison, the reference case (Figure 3-4) is the same in every respect except that it attenuates the heating function by the ratio of package length to 10 m (2.7× greater) producing peak drift-wall temperatures on the order of 460 K (190°C). The temperature rise from 300 K (initial temperature) scales roughly to the value of the “calibration” parameter.



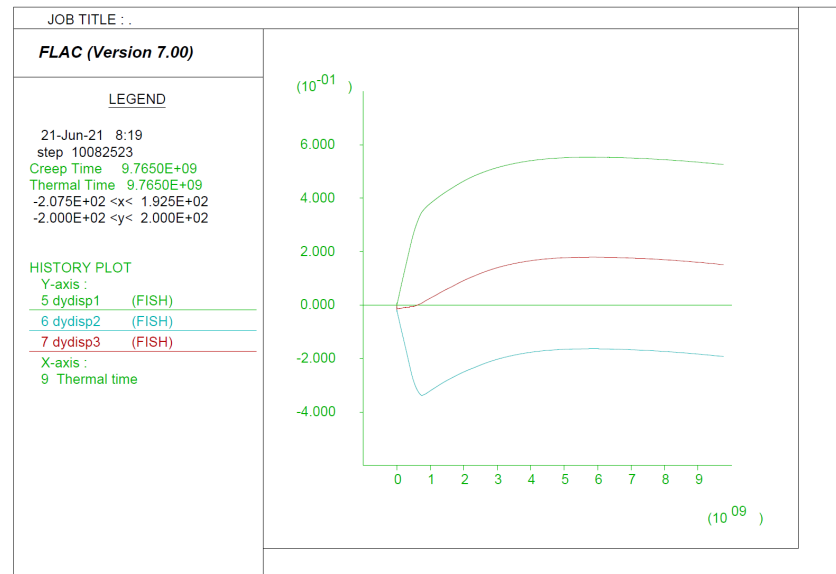
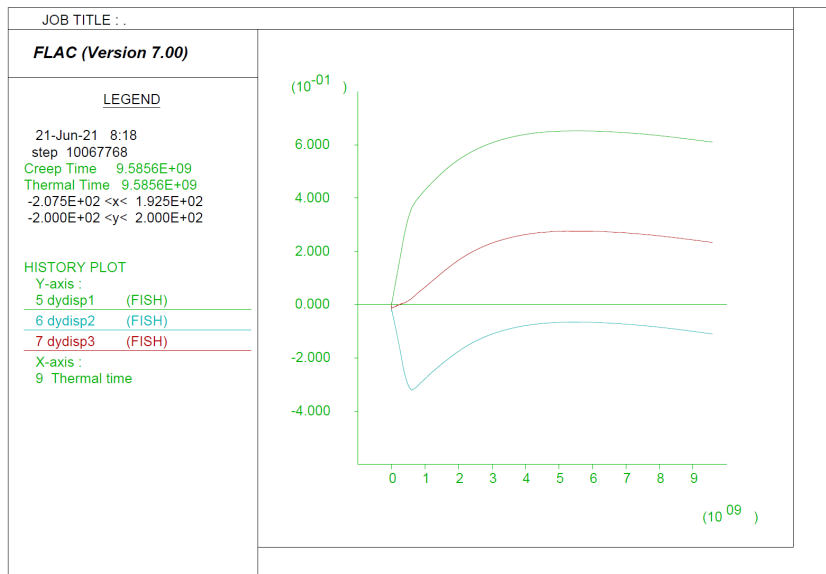
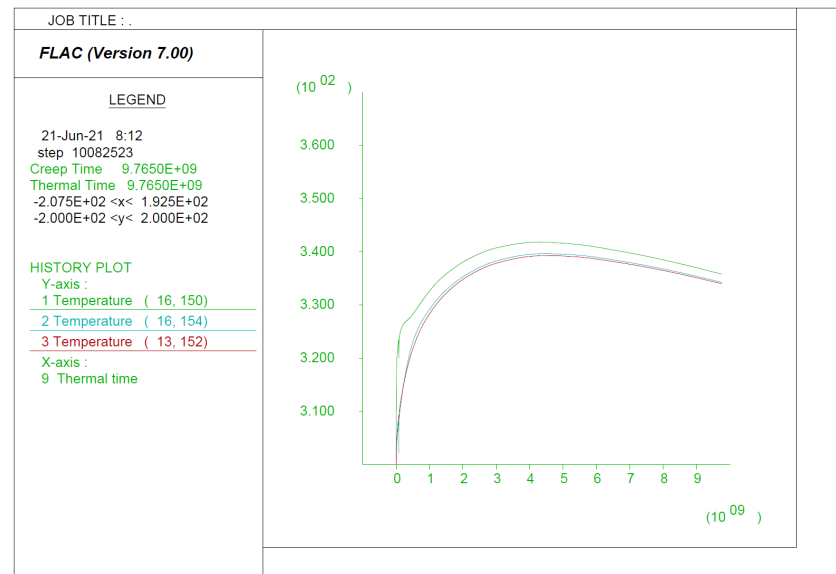
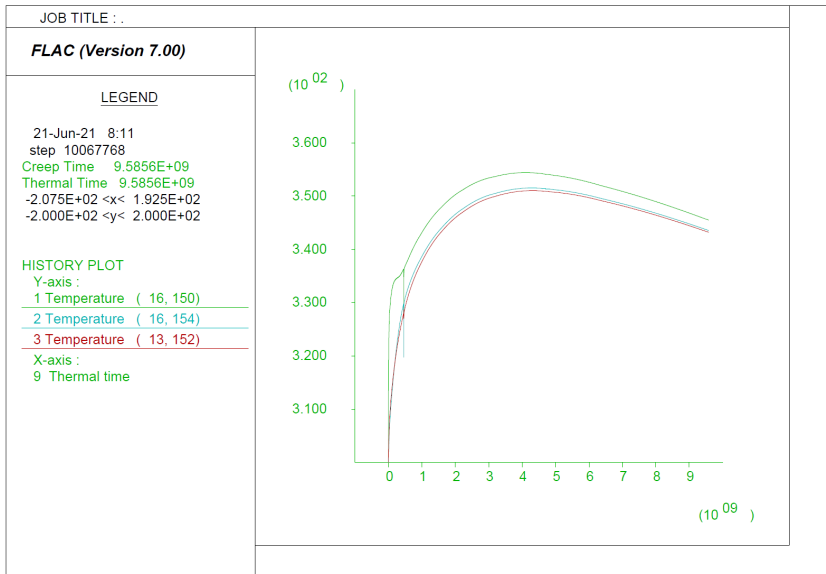


Figure 3-11. Temperature (upper) and y-displacement (lower) for “calibrated” cases with 99<sup>th</sup> (left) and 90<sup>th</sup> (right) percentile heating.

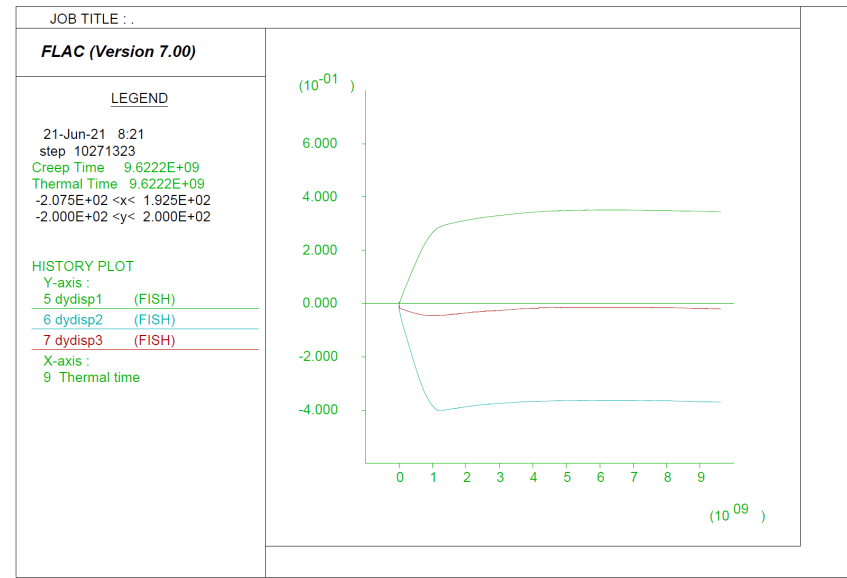
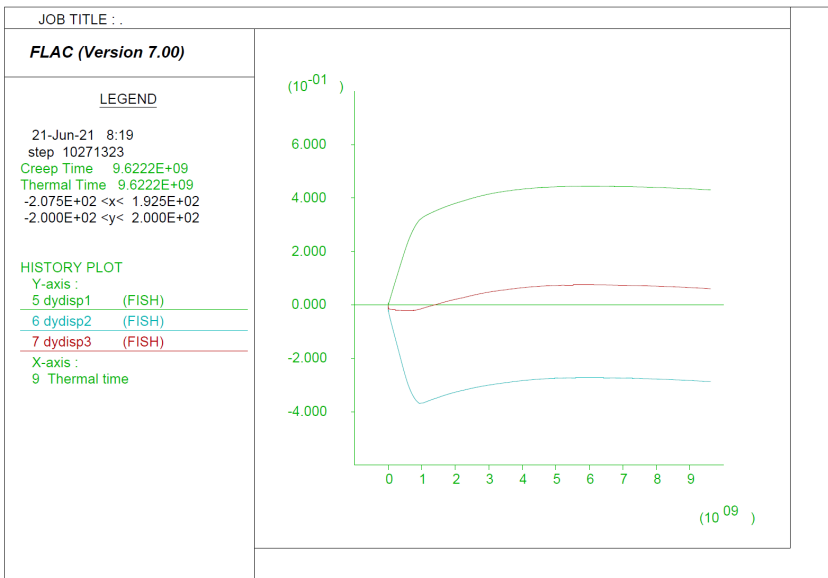
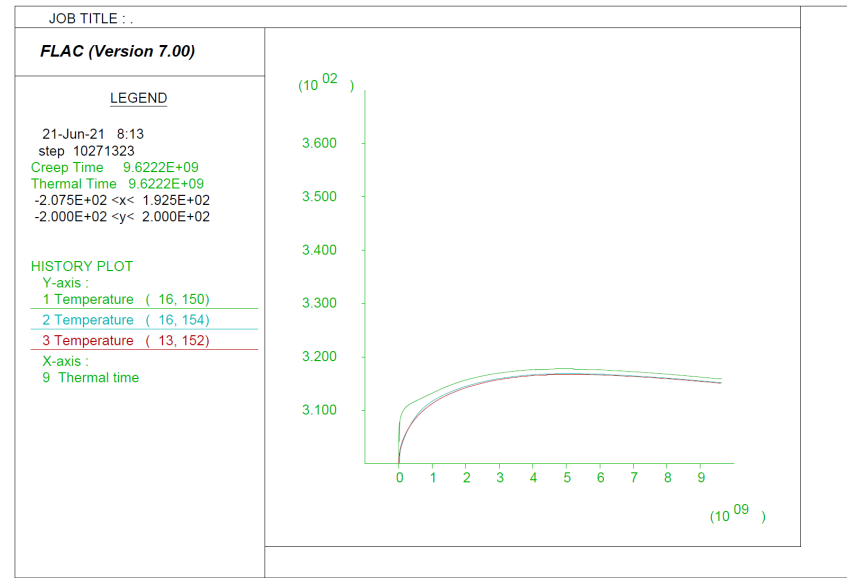
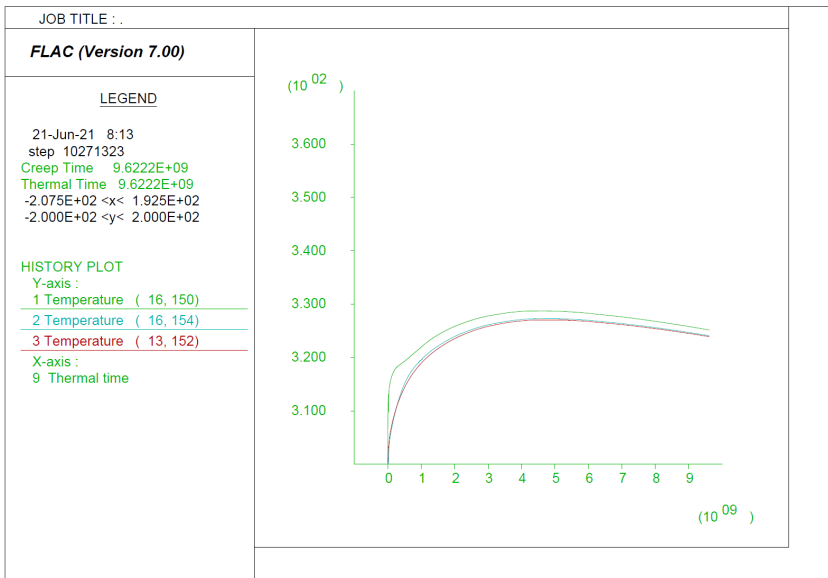


Figure 3-12. Temperature (upper) and y-displacement (lower) for “calibrated” cases with 50<sup>th</sup> (left) and 10<sup>th</sup> (right) percentile heating.

### 3.6 Summary and Recommendations for Thermal-Creep Modeling of Salt

The most important result is that peak repository temperatures calculated using realistic as-loaded DPC thermal output projections, are much lower than for earlier studies that assumed many waste packages filled exclusively with high-burnup SNF.

A secondary result, also important, is that effects from crushed salt backfill consolidation on near-field temperatures are likely to occur before peak temperatures. Thus, near-field peak temperatures remain a key metric for thermal management in a salt repository. In other words, the mechanical details of the crushed salt creep model are of secondary importance to predicting peak near-field temperatures, if nearly complete consolidation occurs within a few decades. This proposition could be confirmed using other creep models such as a Norton-type power law or the Munson-Dawson model (Hardin et al. 2014).

The exception evaluated here is hypothetical, very slow creep (sensitivity analysis shown in Figure 3-7). If backfill consolidation is very slow and takes 100 yr or longer, the overall peak near-field temperature may occur at the waste package during this interval (Figure 3-7). However, the likelihood that thermal activation in the *cwipp* constitutive model (Senseny 1985) is two orders of magnitude too fast, seems remote since the model is based on empirical data including heated tests.

Heat transfer in salt is temperature dependent, and the constitutive relationships ( $K_{th}$  vs.  $T$ ) from Bechthold et al. (2004) are quite important to temperature prediction.

The numerical stability issue with coupled thermal creep (the second case discussed in Section 3.1), and stability of nested grids, could be addressed using a new version of FLAC (e.g., V.8.1). Multi-threading is needed for computational speed for tightening update intervals for coupled properties, and for smaller time steps where needed. The implicit formulation in FLAC, or a finite element code, could also be more stable with coupled property updates.

Grid studies presented in Section 3.4 produced a counter-intuitive result, where the middle grid (0.5 m) temperatures were higher than for both the coarse grid (1 m) and the fine grid (0.25 m). This is interpreted as a combination of numerical diffusion and the effects from the constant-temperature upper and lower boundaries on the model. Both of these explanations affect both the magnitude and timing of peak near-field temperatures. Further grid resolution sensitivity studies are needed with boundaries further distant to more clearly separate intrinsic grid behavior from boundary effects.

## 4. PFLOTRAN Repository Model

This section describes a different modeling approach that includes thermal-hydrologic processes, using the PFLOTRAN code that can also simulate radionuclide release and transport. The immediate motivation for using PFLOTRAN for DPC thermal modeling is to include a mechanistic description of backfill and host rock hydration/dehydration, and the effects on  $K_{th}$  and DPC thermal histories. A longer-term motivation is that regulatory performance assessments are being done using PFLOTRAN, and that future assessments of increasing complexity will continue to be done for DPC-based waste packages.

### 4.1 Natural Barrier System (Host Rock)

#### Shale

Clay-rich sedimentary strata have been considered a potential medium for disposal of radioactive waste in the United States since the forerunner to the DOE introduced a program to develop radioactive waste disposal technology in 1976 (Shurr 1977; Gonzales and Johnson 1985; Rechar et al. 2011). Clay-rich formations are an attractive disposal medium due to

- Low permeability
- High sorption capacity, typically reducing pore-waters (which limit radionuclide solubility)
- Plastically deformable, which promotes self-healing of fractures

Note that clay-rich formations suitable for isolation of radioactive waste span a range of rock types, varying in degree of foliation and degree of consolidation and induration, from unconsolidated mud (such as the Boom Clay) to argillite (such as the Callovo-Oxfordian argillite) (Hansen et al. 2010; Stein et al. 2020; LaForce et al. 2020), but the term “shale” is used somewhat imprecisely to represent all kinds of clay-rich rocks in this report.

#### Crystalline

Characteristics of the crystalline host rock that contribute to or impact post-closure safety include (Mariner et al. 2011; Freeze et al. 2013c):

- The high structural strength of the host rock, which stabilizes engineered barriers
- The depth of burial, which isolates the repository from surface processes (such as erosion and glaciation)
- The low permeability of the host rock, which isolates the repository from surface waters
- The reducing chemical environment, which limits waste package corrosion rates (contributing to waste containment), and limits radionuclide solubility and enhances radionuclide sorption (limiting and delaying radionuclide releases).
- The potential presence of a fracture network that creates a hydraulic connection between the repository and the biosphere, which if present could adversely impact the isolation of the repository and radionuclide releases.

This last characteristic is the primary feature that distinguishes the crystalline reference case from the salt and clay reference cases, in which the host rock is assumed to be a homogeneous medium of uniformly low permeability. In a near-field model, the permeability of the crystalline matrix can

be assumed to be uniformly low by neglecting the presence of fractures or fracture network in a model dimension of interest, but the possibility of long-distance transport through fractures cannot be ignored in a field-scale model.

## **Salt**

Salt's strengths as a host medium for disposal of heat-generating waste are well-known, going back to the 1950s, when geologic salt deposits were first considered promising for radioactive waste disposal (e.g., Hess et al. 1957; Serata and Gloyna 1959; LaForce et al. 2020). The United States has extensive bedded and domal salt deposits (Perry et al. 2014).

The conceptual model includes a mined repository approximately half a kilometer below the surface in a thick bedded salt host rock in a geologically stable sedimentary basin. Characteristics of the bedded salt host rock that contribute to or impact post-closure safety include (Freeze et al. 2013b):

- The ability of salt to creep, which is expected heal fractures, reconsolidate crushed salt backfill, and encapsulate waste, contributing to waste containment; [L]  
[SEP]
- The geologic stability of deep salt beds, which have been isolated from surface processes for hundreds of millions of years, and can be expected to isolate the repository for the duration of the regulatory period; [L]  
[SEP]
- The low permeability (less than  $10^{-20}$  m<sup>2</sup>) and porosity (less than 1.5%) of the host rock, which limits exposure of waste to water, thereby limiting and delaying radionuclide releases; [L]  
[SEP]
- The high thermal conductivity (~5 W/m-K) compared to granite or clay;
- The reducing chemical environment, which limits radionuclide solubility, limiting and delaying radionuclide releases.
- The potential presence of anhydrite interbeds, which are more brittle and of higher permeability than halite, providing potential pathways for radionuclide release.

## **Unsaturated Alluvium**

The safety of an unsaturated zone natural barrier concept relies primarily on the delay and isolation provided by very low recharge rates, low permeability, and distance between a repository and the accessible environment. There is also a reliance on engineered barriers. Siting features in the unsaturated zone generic case that contribute to isolation of waste and delay and (or) limit radionuclide releases include location: [L]  
[SEP]

- Formation thickness – Alluvial fill in basins in the western United States can reach thicknesses on the order of 100s of meters, up to around 1,000 m. Siting a repository in a thick unit isolates waste from and provides longer transport paths to the assessable environment. This feature is also conducive to dual purpose canister disposal. [L]  
[SEP]
- Lower permeability barrier – Alluvial basins tend to have stacked playa and lacustrine sediment deposits located along or near their axes. These units serve to impede migration of radionuclides due to sorption and low permeability, thus providing another mechanism for isolating waste from the assessable environment [L]  
[SEP]

- Low groundwater flux and great depth to water table – Alluvial basins of the western United States are located in arid climates having low to relatively low (under wetter, “ice box” climate conditions documented to have occurred in the past) recharge rates and volumes and high evapotranspiration. These factors result in less potential for groundwater to come into contact with and transport radionuclides within the natural barrier system and helps ensure waste remains isolated from the assessable environment by creating longer transport paths to an aquifer.

The definition of hydrogeologic units is important in conceptualizing and numerically evaluating various natural barrier system scenarios. The alluvial fill of a generic unsaturated zone natural barrier system may be subdivided into two hydrogeologic units: an upper basin-fill aquifer unit representing the upper two-thirds of alluvial fill; and a lower basin fill aquifer unit representing the lower one-third of alluvial fill.

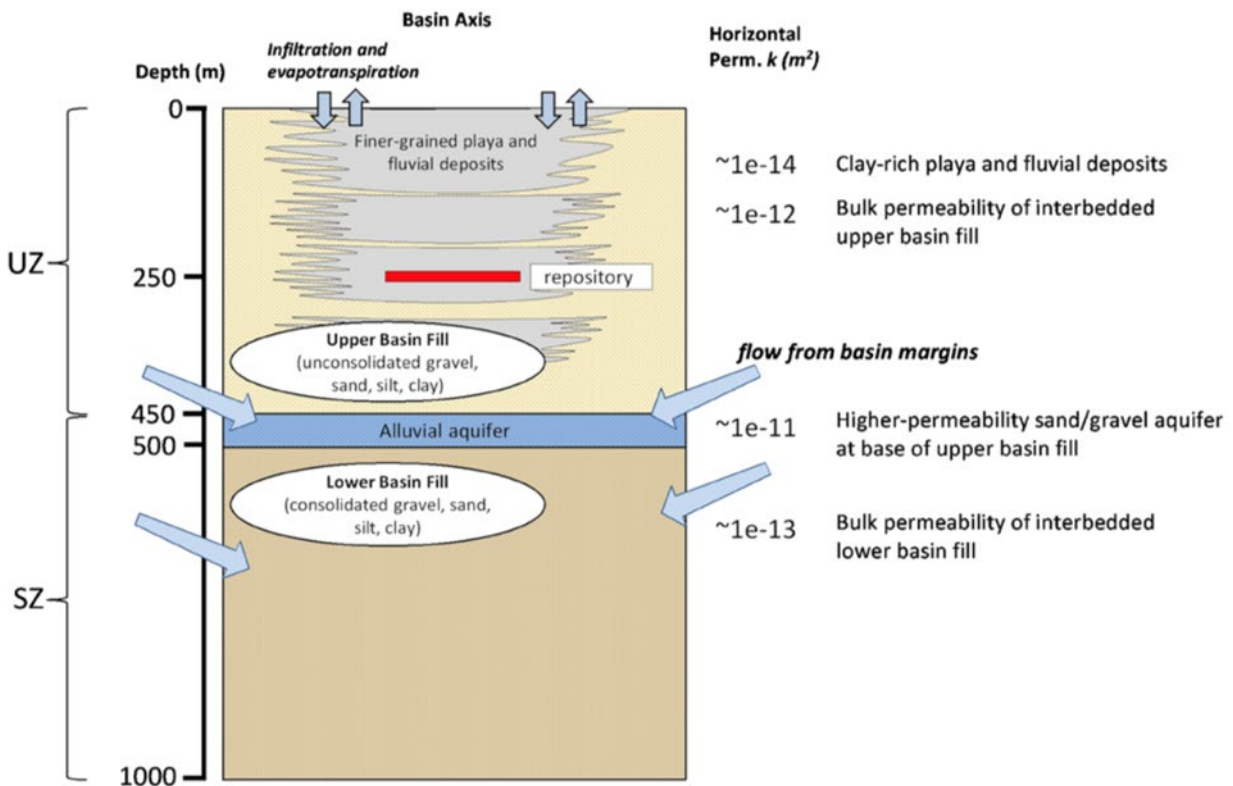


Figure 4-1. Conceptual model of unsaturated alluvium case (after Mariner et al. 2018). The near-field model in this study focuses on the upper UZ portion where the infiltration through the surface is dominant.

The hydrogeologic units in a generic alluvial basin may form two adjoining aquifer systems with confining intervals contained within in the upper aquifer (Mariner et al. 2018). Generally, aquifer materials are higher permeability sand and gravel alluvial fill. Each alluvial aquifer unit may include multiple sheet-shaped water-bearing zones and pod- to tabular- shaped perched water

features on the order of 10s to 100's of meters in lateral extent. Unconsolidated alluvium can have secondary hydraulic conductivity that can enhance or impede fluid flow. The aquifer units are likely stratigraphically and structurally heterogeneous, resulting in a highly variable ability to store and transmit water across the basin. Playa/lacustrine sediment that is part of the upper basin fill aquifer unit is characterized by low permeability, clay-rich, fine-grained sediment and likely has fairly uniform hydraulic properties. The playa and lacustrine deposits tend to be distributed along basin axes as stacked tabular- to pod-shaped features on the order of 10 to 100s of meters in lateral extent.

The near-field model focuses on the UZ portion where the surface infiltration is dominant, and thus, the model domain extends to the surface.

## **4.2 Engineered Barrier System**

### **Bentonite Buffer for Shale and Crystalline Repositories**

Compacted bentonite has low permeability, high sorption capacity, and may be engineered to achieve desirable thermal properties; for instance, quartz sand or graphite can be added to increase thermal conductivity (Choi and Choi 2008; Jobmann and Buntebarth 2009; Wang et al. 2015). The current set of simulations employs a single bentonite buffer with material properties appropriate for a compacted mixture of 70% bentonite and 30% quartz sand. The buffer is assigned a porosity of 0.35 (Liu et al. 2016), a permeability of  $10^{-20}$  m<sup>2</sup> (Liu et al. 2016), and a water-saturated thermal conductivity of 1.5 W/m-K (Wang et al. 2014).

### **Crushed Salt Backfill**

The salt reference case assumes that disposal rooms and access halls are filled with run-of-mine-crushed salt backfill. As summarized in Sevougian et al. (2012, 2013; LaForce et al. 2020), crushed salt backfill is expected to have an initial porosity of approximately 0.35 (Rothfuchs et al. 2003), and correspondingly, permeability higher than and thermal conductivity lower than that of intact salt. See Sections 1 and 3 of this report for more discussion of salt properties. Over time, it will consolidate to a state approaching that of intact salt (Hansen and Leigh 2011, Section 2.4.1.7), a process expected to be mostly complete within approximately 200 years (Clayton et al. 2012).

Following the example of Sevougian et al. (2013), in order to assign properties to the consolidated backfill, it is assumed that the backfill will evolve similarly to a crushed-salt shaft seal. Porosity and permeability values can be drawn from the WIPP parameter database (Fox 2008), which lists two distributions for the porosity and permeability of the shaft seal component in the host rock (“the lower portion of the simplified shaft seal”), one distribution for the first 200 years after emplacement and one for 200-10,000 years after emplacement. The permeability is higher during the initial period, prior to consolidation. The reference case uses the values for the initial 200-year period, because shaft seal consolidation is enhanced at WIPP with the addition of 1 wt. % water (Hansen et al. 2012, Section 4.1.1), which might not be used in run-of- mine backfill.

Backfill is assigned a porosity of 0.026 and a permeability of  $5.6 \times 10^{-21}$  m<sup>2</sup> (Sevougian et al. 2013).

### **Backfill for Unsaturated Alluvium Case**

In this study, buffer section in the model domain does not use properties of specific buffer materials. Instead, backfill and disturbed rock zone (DRZ) sections have the same hydrologic and thermal characteristics, with slight differences in porosity (Mariner et al. 2018).

### 4.3 Waste Package

Waste package porosity is set equal to the fraction of void space within a waste package, which is 50% (Freeze et al. 2013b). Permeability is set several orders of magnitude higher than that of the surrounding materials, so that flow through waste packages is uninhibited. The waste package is given the thermal properties of stainless steel (Shelton 1934).

### 4.4 Numerical Model Setting

#### 4.4.1 Model Domain

The near-field models for different types of geological repositories were run in PFLOTRAN “general” mode solving two-phase (liquid-gas) miscible flow coupled to energy for unsaturated conditions in the waste package, backfill/buffer, DRZ and host rock. Solute transport is excluded in this study. The models simulate a quarter of a single waste package with symmetry conditions at all side boundaries (Figure 4-2).

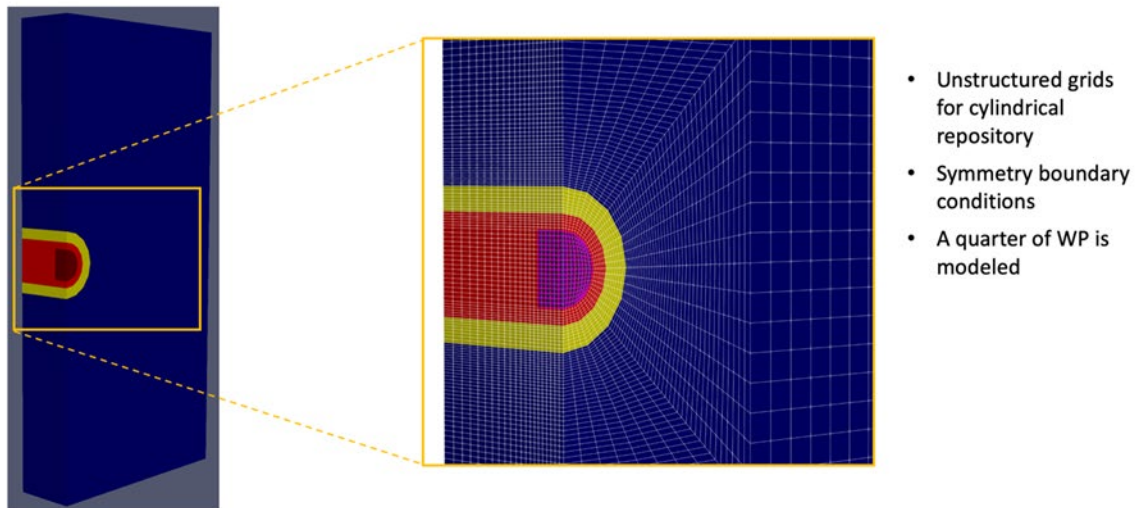


Figure 4-2. Model domain and grid setting. Four sections are modeled: waste package (dark red), backfill/buffer (red), DRZ (yellow), and host rock (blue).

Three concentric sections of waste package, backfill/buffer, and DRZ in the domain of each rock type are modeled according to geometry given in Table 4-1. Assuming that drift geometry for all types of host rock is circular, the circular opening with the radius of each rock is equivalent to the cross-sectional area of the rectangular drifts for the cases that have them. The waste package for shale, crystalline, and salt rock repositories is located at depth of 500 m (middle of the domain in z-direction) and modeled in the domain with height of 75 m (Figure 4-3). For the unsaturated alluvium case, the top of model domain extends to the surface to simulate the effect of infiltration through the surface, and the waste package is located at depth of 250 m.



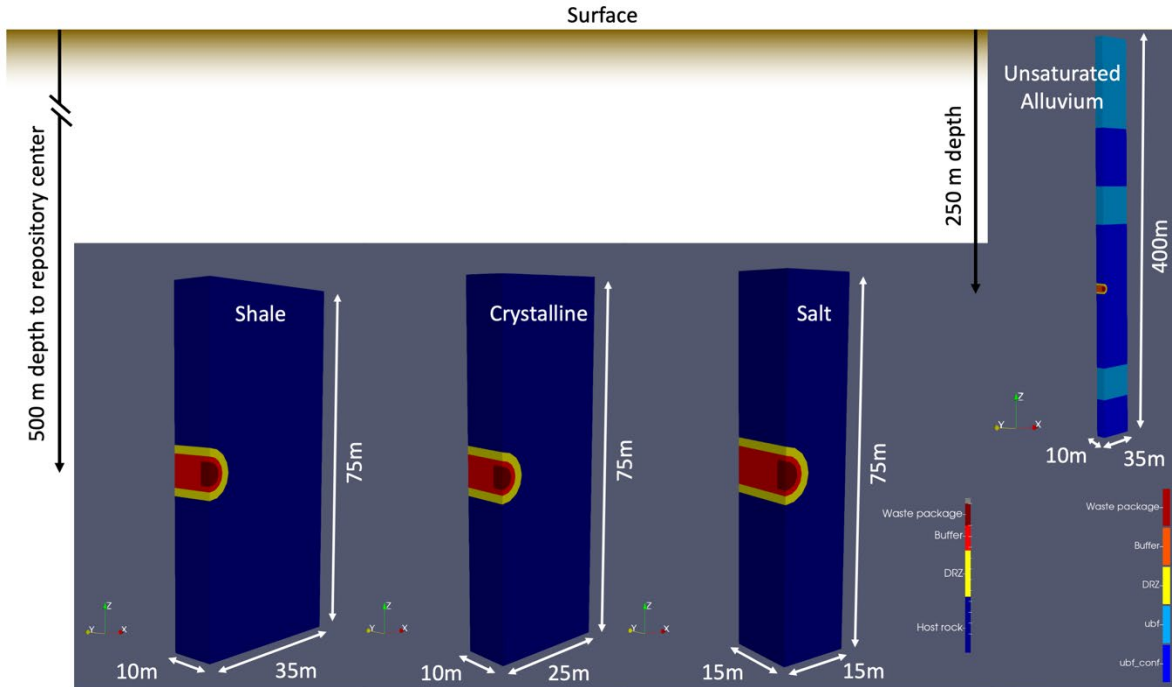


Figure 4-3. Model geometry of four types of repositories. The center of the waste package for shale, crystalline, and salt rock repositories are located at depth of 500m, whereas one for unsaturated alluvium case is located at depth of 250m and the domain top extends to the surface.

#### 4.4.2 Parameters

The material properties of all cases in which permeability and porosity of all formations are constant over time are given in Table 4-1. Shale, crystalline, and salt cases assume homogeneous properties in the domain, whereas the unsaturated alluvium case simulated layered sequences. The backfill/buffer are filled with compacted bentonite for shale and crystalline repositories, whereas salt case uses a crushed salt backfill and UZ uses a crushed alluvium backfill. The DRZ is defined as the portion of the host rock adjacent to the engineered barrier system. Note that mining-induced perturbations in stress state or changes in heating may perturb the thermal properties of the DRZ which is neglected in this study.

For deep repositories of shale, crystalline, and salt rocks, initial fluid pressure and temperature throughout the model domain are calculated by applying hydrostatic and geothermal gradients (10 kPa/m and 0.025°C/m, respectively) in the vertical direction assuming temperature of 18°C and atmospheric pressure at the surface (462.5 m above the top of the model domain).

The shale case assumes the unsaturated condition in the buffer and DRZ, at which initial liquid saturation ( $S_{li}$ ) is set to 0.65 for waste package and buffer, and 0.9 for DRZ, whereas the shale host rock is fully saturated with liquid.

The crystalline and salt cases simulate initial fully-saturated conditions throughout the domain, with the potential for locally unsaturated conditions to result from heating.

Table 4-1. Material parameters for PFLOTRAN modeling.

			Shale	Crystalline	Salt	Unsaturated Alluvium	
<b>Geometry</b>	Radius [m]	WP	2.4	2.25	2.76	2.4	
		Buffer	3.48	3.33	3.84	3.48	
		DRZ	5.15	5	5.51	5.15	
	Spacing [m] Center-to-center	Drift	70	50	30	70	
		Package	20	20	30	20	
Repository depth [m] in model		500	500	500 (to 1000)	250 (>200)		
<b>Permeability [m<sup>2</sup>]</b>		Host rock	1e-19	1e-20	3.1623e-23	<i>Ubf_conf</i>	1e-14
						<i>ubf</i>	1e-12
		DRZ	1e-18	1e-16	3.5813e-17	1e-13	
		Backfill/buffer	1e-20	1e-20	5.62341e-21	1e-13	
<b>Porosity [-]</b>		Host rock	0.2	0.005	0.0182	<i>Ubf_conf</i>	0.4
						<i>ubf</i>	0.4
		DRZ	0.2	0.01	0.0211	0.435	
		Backfill/buffer	0.35	0.35	0.02645	0.4	
<b>Tortuosity</b>		Host rock	0.11	0.2	0.01		
		DRZ	0.11	1.0	0.23	0.63	
		Backfill/buffer	0.23	0.35	0. Note B.02		
<b>Tortuosity function of porosity</b>		Host rock	1.4	Note A.		1.4	
		DRZ	1.4			1.4	
		Backfill/buffer	1.4			1.4	
<b>Soil Compressibility [1/Pa]</b>		Host rock	1.6e-8	2.2e-11	9.747e-11	<i>Ubf_conf</i>	6.4e-8
						<i>ubf</i>	1.6e-8
		DRZ	1.6e-8	2.2e-10	7.41e-10	1.6e-8	
		Backfill/buffer	1.6e-8	1.6e-8	7.41e-10	1.6e-8	
<b>Soil Compressibility function</b>			DEFAULT <sup>B</sup>	DEFAULT	DEFAULT	DEFAULT	
<b>Density [kg/m<sup>3</sup>]</b>		Host rock	2700	2700	2170	<i>Ubf_conf</i>	2700
						<i>ubf</i>	2700
		DRZ	2700	2700	2170	1600	
		Backfill/buffer	2700	2700	2170	2700	
<b>Thermal conductivity (wet) [W/m-K]</b>		Host rock	1.2	2.5	4.9	<i>Ubf_conf</i>	2.0
						<i>ubf</i>	2.0
		DRZ	1.2	2.5	4.9	2.0	
		Backfill/buffer	1.5	1.5	4.8	2.0	
<b>Thermal conductivity (dry)</b>		Host rock	0.6	2.5	4.9	<i>Ubf_conf</i>	1.0
						<i>ubf</i>	1.0
		DRZ	0.6	2.5	4.9	1.0	
		Backfill/buffer	0.6	1.5	4.8	1.0	
<b>Heat capacity</b>		Host rock	830	830	916	<i>Ubf_conf</i>	830
						<i>ubf</i>	830
		DRZ	830	830	916	830	
		Backfill/buffer	830	830	916	830	
<b>Mualem – van Genuchten relative permeability function</b>	Liquid residual saturation	Host rock	0.1	0.1		0.1	
		DRZ					
		Backfill/buffer					
	Gas residual saturation	Host rock	0.1			0.1	
		DRZ					
		Backfill/buffer					
<b>Table continued on next page</b>							

			Shale	Crystalline	Salt	Unsaturated Alluvium
<b>Table 4-1, continued from previous page</b>						
<b>Mualem-Brooks-Corey</b>	Liquid residual saturation	Host rock			0.05	
		DRZ				
		Backfill/buffer				
	Lamda	Host rock			0.5	
		DRZ				
		Backfill/buffer				
<b>Van Genuchten saturation function</b>	Alpha [1/Pa]	Host rock	6.67e-7	1e-4	1e-3	1e-3
		DRZ				
		Backfill/buffer				
	m	Host rock	0.333	0.5	0.75	0.5
		DRZ				
		Backfill/buffer				
<b>Diffusion coefficient [m<sup>2</sup>/s]</b>		Liquid	1e-9	1e-9	2.3e-9	1e-9
		Gas	2.1e-5			2.1e-5
<b>Initial gas saturation [-]</b>		Host rock	0.0	0.0	0.0	Vary
		DRZ	0.35	0.0	0.0	0.7
		Backfill/buffer	0.35	0.0	0.0	0.7
Notes:						
A. Shaded areas of table are not applicable.						
B. PFLOTRAN default parameter value.						

For the unsaturated alluvium case, initial pressure, temperature, and gas/liquid saturation are set according to the material properties based on the layered system (Figure 4-4).

All of the simulations run 10<sup>4</sup> years.

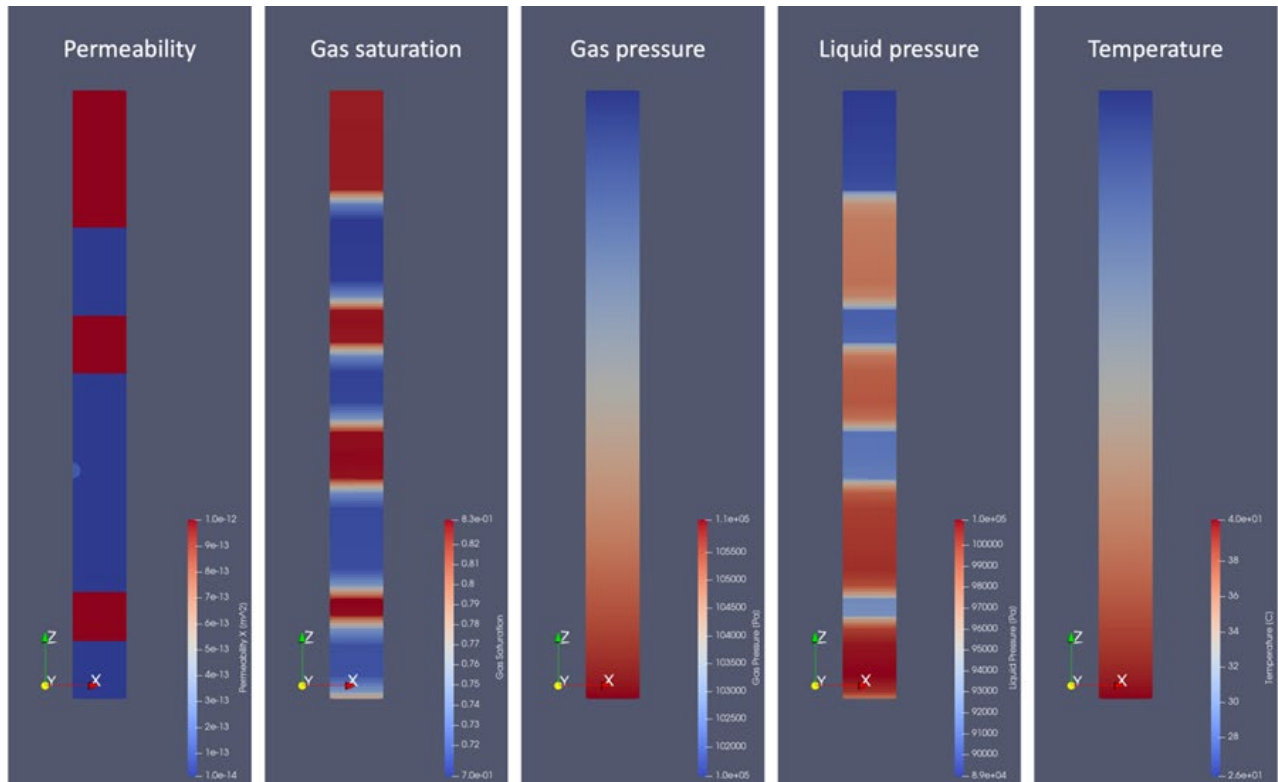


Figure 4-4. Initial conditions for unsaturated alluvium case.

## 4.5 Results

In this study, near-field PFLOTRAN models simulate the 90<sup>th</sup> and 50<sup>th</sup> percentile DPC heat sources for four types of repositories (shale, crystalline, salt, and unsaturated alluvium).

Figure 4-5 shows the temporal evolution of temperature (Figures 4-5a to 4-5c), liquid pressure (4-5d to 4-5f) and gas pressure/saturation (4-5g to 4-5i) within waste package (left), backfill/buffer (middle), and DRZ (right) for shale (black), crystalline (green), salt (orange), and unsaturated alluvium (blue) host rocks.

For the shale case, the large capillary entry pressure initially generates large negative liquid pressure within the buffer (Figure 4-5e). Swelling, driven by ingress of moisture, causes the buffer and DRZ to saturate with time (gas saturation goes to zero; Figure 4-5h).

The crystalline case shows intermediate temperature and pressure evolution according to its hydraulic and thermal characteristics. Note that the crystalline rock will impose multi-scale fractures in nature, but their impacts on near-field behaviors may be negligible in a relatively short-term as this study assumes.

The salt rock has the lowest permeability but largest thermal conductivity, which results in the smallest increases in temperature at given heat source (Figures 4-5a to 4-5c).

Note that where temperature does not exceed boiling, a gas phase may not develop. The crystalline and salt cases show evidence of this (green and orange traces in the lower tiers of Figure 4-5 and 4-6).

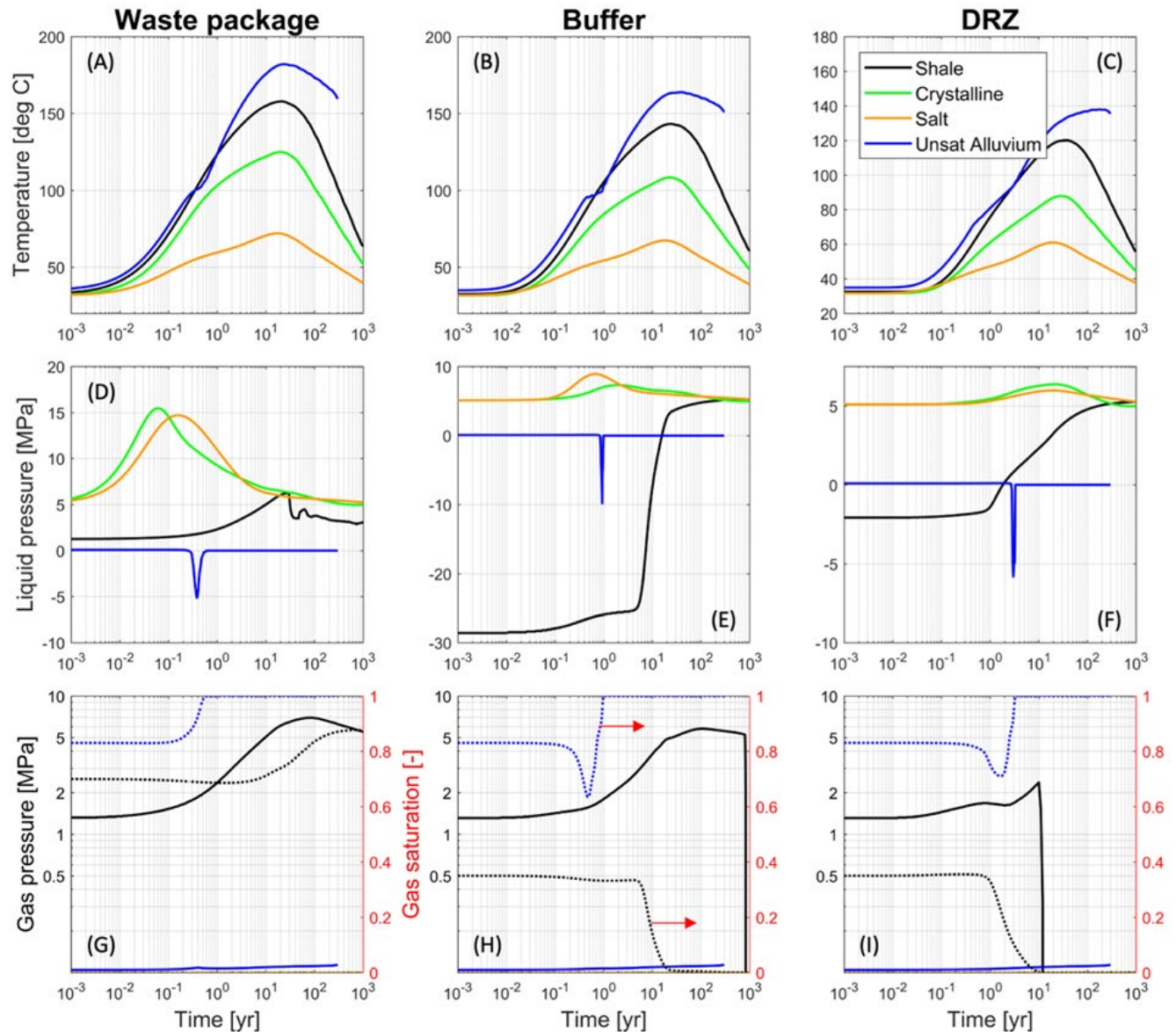


Figure 4-5. Results for the 90<sup>th</sup> percentile DPC heat source: (A to C) temperature; (D to F) liquid pressure; and (G to I) gas pressure and saturation.

For the unsaturated alluvium case, dewatering and the layered system with confining units retard heat transport out of the host unit where the waste package is located, which produces higher temperatures that persist longer than for other cases (Figures 4-5a to 4-5c). Thus, the whole domain is initially unsaturated with smaller pressure gradient, but subsequent heat causes fully gas-saturated conditions at early stage (less than 1 year; Figures 4-5g to 4-5i).

With total vertical domain height of 75 m (repository in the middle), the shale, crystalline, and salt models presented here probably are being cooled by these constant-temperature boundaries after

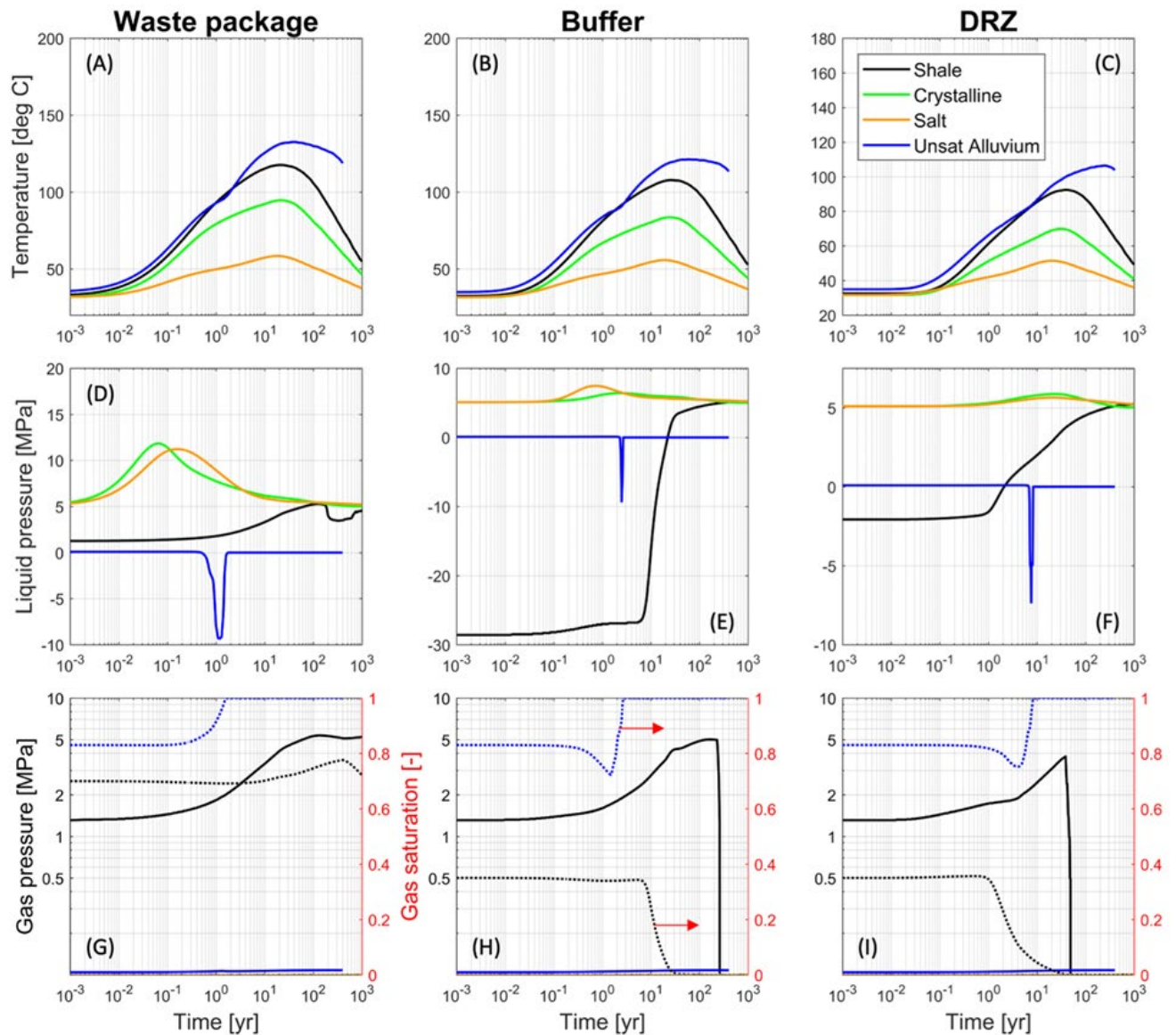


Figure 4-6. Results for the 50<sup>th</sup> percentile DPC heat source: (A to C) temperature; (D to F) liquid pressure; and (G to I) gas pressure and saturation.

a few decades of simulation time. Future work will evaluate the vertical domain as discussed in Section 3 and noted in Section 5.

The lower heat source (50%) reduces the maximum temperature and pressure fields in all cases. For the shale case, faster swelling gives faster resaturation of the buffer and DRZ due to less heating.

Note that the results from unsaturated alluvium case stop after 400-years of simulation time. This is likely because the PFLTRAN default solvers have difficulty converging during the dryout and

resaturation processes and was also observed in PA-scale unsaturated alluvium simulations in Sevougian et al (2019). The gravity-driven behavior of the flow is also not properly solved by the current PFLOTRAN. An example of erroneous gas saturation distorted by the unstructured grid is shown in Figure 4-7. Further work on the UZ mesh and updated PFLOTRAN solvers will be required to complete the UZ simulation.

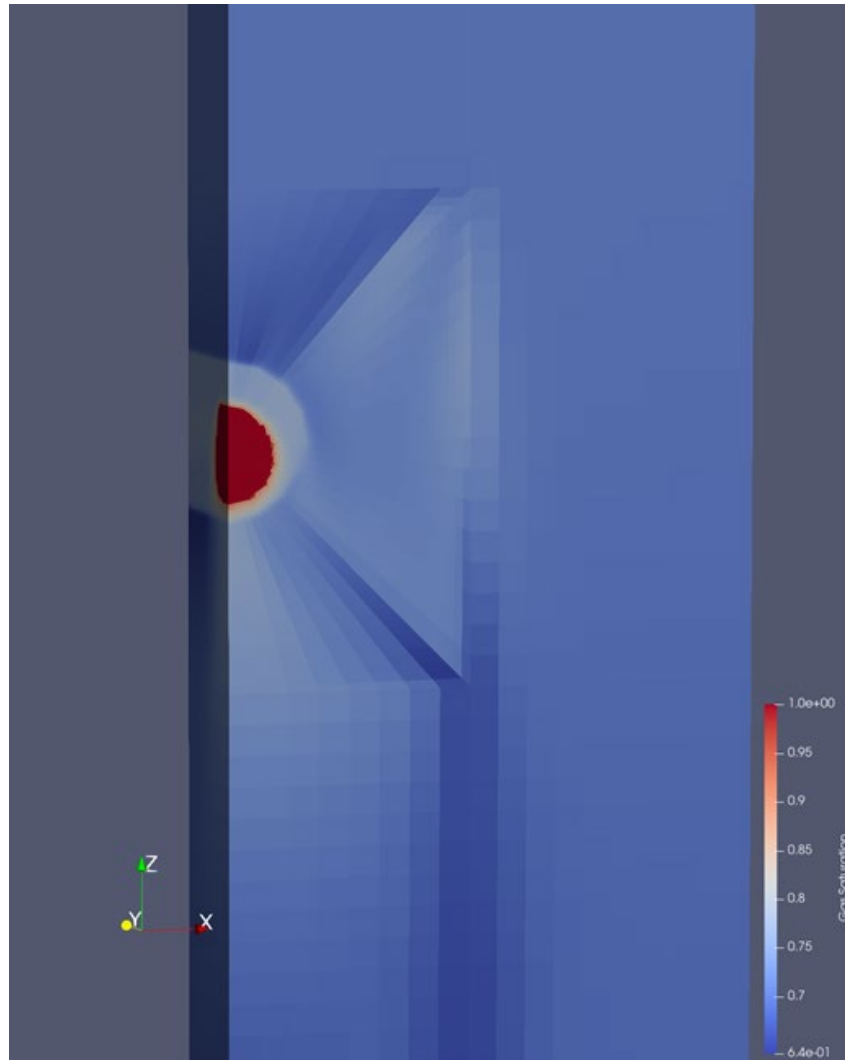


Figure 4-7. Odd behaviors of flow within unstructured grids: gas saturation.

## 5. Summary and Recommendations

This is a progress report on thermal modeling for DPC direct disposal, that covers several available calculation methods and addresses creep and temperature-dependent properties in a salt repository. Three modeling approaches are demonstrated (Sections 2, 3 and 4). They are at different levels of maturity, and future work is expected to add refinements and establish the best applications for each.

The principal take-away is that the near-field temperatures at or near DPC-based waste packages are much lower than previous studies have suggested. This is because the present study exclusively uses thermal output projections for as-loaded DPCs from the UNF-ST&DARDS database, whereas previous studies have used bounding assumptions, such that for the hottest cases all waste packages contain high-burnup fuel of young age. This finding requires that waste package emplacement in a repository begin at or around calendar 2100, so that each DPC ages about 100 yr before disposal.

Recommendations for future work are presented:

- A numerical 3D model would be useful to validate or replace the semi-analytical model.
- Various sensitivity studies and model upgrades are suggested for coupled thermal creep modeling (Section 3.6).
- Additional grid refinements and vertical domain sensitivity studies would be useful for PFLOTRAN modeling.
- Grid resolution studies and sensitivity studies (e.g., unsaturated hydrologic properties) would also be helpful for PFLOTRAN modeling.
- Additional simulations with alternative aging/emplacement schedules (e.g., other repository start dates) are suggested.

It is anticipated that after some further development, these models will be used to develop high-confidence thermal histories for the outer surfaces of DPC-based waste packages. These would then be used as boundary conditions for internal heat transfer models of the DPCs, to develop histories for fuel rods and other components after disposal.



## 6. References

- Banerjee, K., K.R. Robb, G. Radulescu, J.M. Scaglione, J.C. Wagner, J.B. Clarity, R.A. LeFebvre and J.L. Peterson 2016. "Estimation of Inherent Safety Margins in Loaded Commercial Spent Nuclear Fuel Casks," *Nuclear Technology*. 195:2, p. 124-142.
- Bechthold, W., E. Smailos, S. Heusermann, W. Bollingerfehr, B. Bazargan Sabet, T. Rothfuchs, P. Kamlot, J. Grupa, S. Olivella, and F.D. Hansen 2004. *Backfilling and Sealing of Underground Repositories for Radioactive Waste in Salt (BAMBUS II Project), Final Report*. EUR 20621, Nuclear Science and Technology, Luxembourg.
- Choi, H. J. and J. Choi 2008. "Double-layered buffer to enhance the thermal performance in a high-level radioactive waste disposal system." *Nuclear Engineering and Design*. V. 238, N. 10, pp. 2815-2820.
- Clarity, J., K. Banerjee, H.K. Liljenfeldt and W.J. Marshall 2017 "As-Loaded Criticality Margin Assessment of Dual-Purpose Canisters Using UNF-ST&DARDS." *Nuclear Technology*. 199:3, pp. 245-275.
- Clayton, D.J., J.G. Arguello Jr., E.L. Hardin, F.D. Hansen, and J.E. Bean 2012. "Thermal-Mechanical Modeling of a Generic High-Level Waste Salt Repository." In: *SALTVII, 7th Conference on the Mechanical Behavior of Salt*. Paris, France. April 16-19, 2012. Sandia National Laboratories, Albuquerque, NM (SAND2012- 2741 C).
- Freeze, G., S.D. Sevougian and M. Gross 2013a. *Safety Framework for Disposal of Heat-Generating Waste in Salt: Features, Events, and Processes (FEPs) Classification*. FCRD-UFD-2013-000191. Office of Used Nuclear Fuel Disposition, U.S. Department of Energy. Sandia National Laboratories, Albuquerque, NM (SAND2013-5220 P).
- Freeze, G., W.P. Gardner, P. Vaughn, S.D. Sevougian, P. Mariner, V. Mousseau and G. Hammond 2013b. *Enhancements to the Generic Disposal System Modeling Capabilities*. FCRD-UFD-2014-000062. Office of Used Nuclear Fuel Disposition, U.S. Department of Energy. Sandia National Laboratories, Albuquerque, NM (SAND2013-10532 P).
- Freeze, G., M. Voegele, P. Vaughn, J. Prouty, W.M. Nutt, E. Hardin and S.D. Sevougian 2013c. *Generic Deep Geologic Disposal Safety Case*. FCRD-UFD-2012-000146 Rev. 1. Office of Used Nuclear Fuel Disposition, U.S. Department of Energy. (SAND2013- 0974 P)
- Gonzales, S. and K.S. Johnson 1984. *Shale and other argillaceous strata in the United States*. Oak Ridge National Laboratory. ORNL/Sub/84-64794/1.
- Hansen, F.D., E.L. Hardin, R.P. Rechar, G.A. Freeze, D.C. Sassani, P.V. Brady, C.M. Stone, M.J. Martinez, J.F. Holland, T. Dewers, K.N. Gaither, S.R. Sobolik and R.T. Cygan 2010. *Shale Disposal of U.S. High-Level Radioactive Waste*. SAND2010-2843. Sandia National Laboratories, Albuquerque, New Mexico.
- Hansen, F. D. and C.D. Leigh 2011. *Salt Disposal of Heat-Generating Nuclear Waste*. SAND2011-0161. Sandia National Laboratories, Albuquerque, NM.

Hansen F. D., S. J. Bauer, S. T. Broome, and G. D. Callahan 2012. *Coupled Thermal-Hydrological- Mechanical Processes in Salt: Hot Granular Salt Consolidation, Constitutive Model and Micromechanics*. FCRD-USED-2012-000422. Office of Used Nuclear Fuel Disposition, U.S. Department of Energy. Sandia National Laboratories, Albuquerque, NM (SAND2012-9893 P).

Hardin, E., J. Blink, H. Greenberg, M. Sutton, M. Fratoni, J. Carter, M. Dupont and R. Howard 2011. *Generic Repository Design Concepts and Thermal Analysis (FY11)*. FCRD-USED-2011-000143 Rev. 2. Used Fuel Disposition R&D Campaign, U.S. Department of Energy.

Hardin, E., T. Hadgu, D. Clayton, R. Howard, H. Greenberg, J. Blink, M. Sharma, M. Sutton, J. Carter, M. Dupont, and P. Rodwell. 2012a. *Repository Reference Disposal Concepts and Thermal Management Analysis*. FCRD-USED-2012-000219 Rev. 2. Office of Used Nuclear Fuel Disposition, U.S. Department of Energy.

Hardin, E., T. Hadgu, H. Greenberg and M. Dupont 2012b. *Parameter Uncertainty for Repository Thermal Analysis*. FCRD-UFD-2012-000097. Used Fuel Disposition R&D Campaign, U.S. Department of Energy.

Hardin, E.L. 2013. *Temperature-Package Power Correlations for Open-Mode Geologic Disposal Concepts*. SAND2013-1425. Sandia National Laboratories, Albuquerque, NM.

Hardin, E.L., D.J. Clayton, M.J. Martinez, G. Nieder-Westermann, R.L. Howard, H.R. Greenberg, J.A. Blink and T.A. Buscheck 2013. *Collaborative Report on Disposal Concepts*. FCRD-UFD-2013-000170 Rev. 0. Used Fuel Disposition R&D Campaign, U.S. Department of Energy.

Hardin, E., K. Kuhlman and F. Hansen 2014. *Measuring Low-Stress, Low Strain-Rate Deformation Relevant to a Salt Repository*. FCRD-UFD-2014-000614 Rev. 0. Office of Used Nuclear Fuel Disposition, U.S. Department of Energy.

Hardin, E.L., L. Price, E. Kalinina, T. Hadgu, A. Ilgen, C. Bryan, J. Scaglione, K. Banerjee, J. Clarity, R. Jubin, V. Sobes, R. Howard, J. Carter, T. Severynse, and F. Perry 2015. *Summary of Investigations on Technical Feasibility of Direct Disposal of Dual-Purpose Canisters*. FCRD-UFD-2015-000129 Rev 0. Office of Used Nuclear Fuel Disposition, U.S. Department of Energy.

Hess, H.H., J.N. Adkins, W.B. Heroy, W.E. Benson, M.K. Hubbert, J.C. Frye, R.J. Russell & C.V. Theis, 1957. "The Disposal of Radioactive Waste on Land." Publication 519: *Report of the Committee on Waste Disposal of the Division of Earth Sciences*. U.S. National Academy of Sciences.

Itasca (Itasca Consulting Group) 2011. *FLAC Version 7.00 User's Guide*. Minneapolis, MN.

Jobmann, M. and G. Buntebarth 2009. "Influence of graphite and quartz addition on the thermo-physical properties of bentonite for sealing heat-generating radioactive waste." *Applied Clay Science*. V. 44, N. 3- 4, pp. 206-210.

LaForce, T., K.W. Chang, F.V. Perry, T.S. Lowry, E. Basurto, R. Jayne, D. Brooks, S. Jordan, E. Stein, R. Leone and M. Nole 2020. *GDSA Repository Systems Analysis Investigations in FY2020*. M2SF-20SN010304052. Office of Spent Fuel and Waste Science & Technology, U.S. Department of Energy. SAND2020-12028 R. Sandia National Laboratories, Albuquerque, NM.

- Liu, J. F., Y. Song, F. Skoczylas and J. Liu 2016. "Gas migration through water-saturated bentonite-sand mixtures, COX argillite, and their interfaces." *Canadian Geotechnical Journal*. V. 53, N. 1, pp. 60-71.
- Mariner, P.E., J.H. Lee, E.L. Hardin, F. D. Hansen, G. A. Freeze, A.S. Lord, B. Goldstein and R.H. Price 2011. *Granite Disposal of U.S. High-Level Radioactive Waste*. Sandia National Laboratories, Albuquerque, NM (SAND2011-6203).
- Mariner, P.E., E.R. Stein, J.M. Frederick, S.D. Sevougian and G.E. Hammond 2018. *Advances in Geologic Disposal Safety Assessment and an Unsaturated Alluvium Reference Case*. SFWD-SFWST-2018-000509. Office of Spent Fuel and Waste Science & Technology, U.S. Department of Energy. SAND2018-11858R. Sandia National Laboratories, Albuquerque, NM.
- Perry, F.V., R.E. Kelley, P.F. Dobson and J.E. Houseworth 2014. *Regional Geology: A GIS Database for Alternative Host Rocks and Potential Siting Guidelines*. FCRD-UFD-2013-000068. Office of Used Nuclear Fuel Disposition, U.S. Department of Energy. Los Alamos National Laboratory (LA-UR-14- 20368).
- Rechard, R.P., B. Goldstein, L.H. Brush, J.A. Blink, M. Sutton, and F.V. Perry 2011. *Basis for Identification of Disposal Option for Research and Development for Spent Nuclear Fuel and High-Level Waste*. FCRD-USED-2011-000071. Used Fuel Disposition Campaign, U.S. Department of Energy. Sandia National Laboratories, Albuquerque NM (SAND2011-3781P).
- Robinson, E.C. 1988. *Thermal Properties of Rocks*. USGS Open File Report 88-441. U.S. Geological Survey.
- Rothfuchs, T., K. Wieckzorek, B. Bazargan and S. Olivella 2003. "Results of the BAMBUS II Project – Experimental and Modelling Results concerning Salt Backfill Compaction and EDZ Evolution in a Spent Fuel Repository in Rock Salt Formations." Eurosafe Forum. Paris, November 25-26, 2003. [www.eurosafe-forum.org](http://www.eurosafe-forum.org)
- Senseny, P.E. 1985. "Determination of a Constitutive Law for Salt at Elevated Temperature and Pressure." *Measurement of Rock Properties at Elevated Pressures and Temperatures* (H.J. Pincus and E.R. Hoskins, eds.). American Society for Testing and Materials, Special Technical Publication 869. Philadelphia, PA.
- Serata, S. and E.F. Gloyne 1959. *Development of Design Principle for Disposal of Reactor Fuel Waste into Underground Salt Cavities*. Atomic Energy Commission.
- Sevougian, S.D., G.A. Freeze, M.B. Gross, J. Lee, C.D. Leigh, P. Mariner, R.J. MacKinnon, and P. Vaughn 2012. *TSPA Model Development and Sensitivity Analysis of Processes Affecting Performance of a Salt Repository for Disposal of Heat-Generating Nuclear Waste*. FCRD-UFD-2012-000320 Rev. 0. Office of Used Nuclear Fuel Disposition, U.S. Department of Energy.
- Sevougian, S.D., G.A. Freeze, P. Vaughn, P. Mariner, and W.P. Gardner 2013. *Update to the Salt R&D Reference Case*. FCRD-UFD-2013-000368. Office of Used Nuclear Fuel Disposition, U.S. Department of Energy. (SAND2013-8255 P)
- Sevougian, S.D., E.R. Stein, T. LaForce, F.V. Perry, M. Nole and K.W. Chang 2019. *GDSA Repository Systems Analysis FY19 Update*. M3SF-19SN010304052. Office of Spent Fuel and Waste Science & Technology. SAND2019-11942R. Sandia National Laboratories, Albuquerque, NM.

Shurr, G.W. (1977), *The Pierre Shale, Northern Great Plains: A Potential Isolation Medium for Radioactive Waste*. Open-File Report. United States Geological Survey. Reston, VA: 27.

SNL (Sandia National Laboratories) 2019. *A Salt Repository Concept for CSNF in 21-PWR Size Canisters*. SFWD-IWM-2017-000246 Rev. 2. Office of Spent Fuel and Waste Disposition, Integrated Waste Management, U.S. Department of Energy.

SNL (Sandia National Laboratories) 2020. *DPC Disposal Concepts of Operations*. M3SF-20SN010305052 Rev. 1. Office of Spent Fuel and Waste Disposition, Integrated Waste Management, U.S. Department of Energy. Sandia National Laboratories, Albuquerque NM (SAND2020-2901 R).

Stein et al. 2020. *Disposal Concepts for a High-Temperature Repository in Shale*. M3SF-21SN010304064. Office of Spent Fuel and Waste Science and Technology, U.S. Department of Energy. Sandia National Laboratories, Albuquerque NM (SAND2020-12471 R).

Sutton, M., J.A. Blink, M. Fratoni, H.R. Greenberg and A.D. Ross 2011. *Investigations on Repository Near-Field Thermal Modeling – Repository Science/Thermal Load Management & Design Concepts (M41UF033302 Rev. 1)*. LLNL-TR-491099-REV-1. Lawrence Livermore National Laboratory.

Wang, Y., T. Hadgu, E. Matteo, J. N. Kruichak, M. M. Mills, R. Tinnacher, J. Davis, H. S. Viswanathan, S. Chu, T. Dittrich, F. Hyman, S. Karra, N. Makedonska, P. Reimus, M. Zavarin, P. Zhao, C. Joseph, J. B. Begg, Z. Dai, A. B. Kersting, J. Jerden, J. M. Copple, T. Cruse and W. Ebert 2015. *Used Fuel Disposal in Crystalline Rocks: FY15 Progress Report*. FCRD-UFD-2015-000125. Office of Used Fuel Disposition, U.S. Department of Energy.